

A new genus of Rhinocerotidae (Mammalia, Perissodactyla) from the Oligocene of Europe

Damien Becker^{a*}, Pierre-Olivier Antoine^b and Olivier Maridet^c

^aSection d'archéologie et paléontologie, République et Canton du Jura, Office Cantonal de la Culture, Hôtel des Halles, PO Box 34, CH-2900, Porrentruy, Switzerland; ^bInstitut des Sciences de l'Evolution, Université Montpellier 2, Place Eugène Bataillon, F-34095 Montpellier, France; ^cKey Laboratory of Evolutionary Systematics of Vertebrates, Institute of Vertebrate Paleontology and Paleoanthropology, Chinese Academy of Sciences, 142 Xizhimenwai Dajie, PO Box 643, Beijing 100044, PR China

(Received 4 October 2011; accepted 18 January 2012; first published online 22 March 2013)

A newly discovered, well-preserved skull and associated fragment of a juvenile mandible from the Early Oligocene locality of Poillat (Canton Jura, NW Switzerland), bearing close affinities with the rhinocerotid *Protaceratherium albigense* (Roman, 1912), are attributed to a new small-sized representative of early diverging Rhinocerotinae, *Molassitherium delemontense* gen. et sp. nov. Other specimens from Western Europe, formerly questionably referred to *Epiaceratherium* Abel, 1910, are assigned to this new genus. Comparison with the previously described *Protaceratherium* Abel, 1910 (including type material) and a phylogenetic analysis highlight the mismatch of *Protaceratherium minutum* (Cuvier, 1822) and *Protaceratherium albigense* (Roman, 1912). Given the topology of the most parsimonious tree, a basal split within Rhinocerotidae coincides with the well-supported divergence of the Elasmotheriinae and Rhinocerotinae clades. Relationships within Rhinocerotinae are [*Epiaceratherium bolcense* Abel, 1910 [*Epiaceratherium magnum* Uhlig, 1999 [*Molassitherium* gen. nov. [*Mesaceratherium* Heissig, 1969 [*Pleuroceros* Roger, 1898 [*Protaceratherium minutum* (Cuvier, 1822) [*Plesiaceratherium mirallesi* (Crusafont, Villalta and Truyols, 1955) [*Aceratheriini*, Rhinocerotini]]]]]]]]. The only paraphyletic genus in the analysis is *Epiaceratherium*, with the earliest Oligocene *Epiaceratherium bolcense* Abel, 1910 being sister taxon to an [*Epiaceratherium magnum* Uhlig, 1999, Rhinocerotinae] clade. In the single most parsimonious tree, *Molassitherium* gen. nov., included within the early diverging Rhinocerotinae, forms a clade encompassing *Molassitherium delemontense* gen. et sp. nov. and the type species *Molassitherium albigense* comb. nov. The range of *Molassitherium delemontense* gen. et sp. nov. is so far restricted to the late Early–early Late Oligocene interval in Western Europe (Germany, Switzerland, France; ‘late MP22’–MP25).

<http://zoobank.org/urn:lsid:zoobank.org:pub:0A6A2A39-719A-40A1-96B8-ABB25F02C03E>

Keywords: Rhinocerotinae; *Molassitherium delemontense* gen. et sp. nov.; cladistics; biostratigraphy; Jura Molasse; Switzerland

Introduction

Abel (1910) established the genus *Protaceratherium* for the small slender rhinoceros *P. minutum* (Cuvier, 1822) from the Early Miocene of Europe, previously assigned to *Diceratheriinae* Dollo, 1885 under the name *Diceratherium minutum* by Osborn (1900). Roman (1912) described the species *Acerotherium albigense*, reassessed as *P. albigense* by von Breuning (1924), on the basis of an anterior part of an adult skull, with preserved left and right P1–M3, discovered in the molassic deposits of the early Late Oligocene of La Sauzière Saint-Jean (MP25–26; SW France). The affinities and the suprageneric assignment of *Protaceratherium* species have been discussed for a long time. Heissig (1969) considered them as *Dicerorhininae* Simpson, 1945, likewise Spillmann (1969), who even suggested *Protaceratherium* as junior synonym of *Diceratherium* Marsh, 1875 (*Dicerorhininae*), whereas Cerdeño (1995)

proposed a synonymy with *Plesiaceratherium* Young, 1937 (*Aceratheriinae* Dollo, 1885). On the other hand, Heissig (1973) was indecisive between *Caenopinae* Cope, 1887 and *Aceratheriinae* but suggested in 1989 assignment to *Menoaceratini* Prothero *et al.*, 1986, which he considered as a tribe within *Aceratheriinae*. Indeed, many authors have regularly attributed the genus *Protaceratherium* to the subfamily *Aceratheriinae* (e.g. von Breuning 1924; Huguéney & Guérin 1981; Ménouret & Guérin 2009), as opposed to Antoine *et al.* (2003b) who assigned *P. minutum* to the tribe *Rhinocerotini* (*Rhinocerotinae*). Recently, Lihoreau *et al.* (2009) and Antoine *et al.* (2010) placed both *P. albigense* and *P. minutum* in *Rhinocerotinae incertae sedis*. Through a morphology-based phylogenetic analysis devoted to other rhinocerotids, Antoine *et al.* (2010) argued that *P. albigense* was set well apart from the type species of the genus (*P. minutum*), without proposing any nomenclatural change for the former species.

*Corresponding author. Email: damien.becker@jura.ch

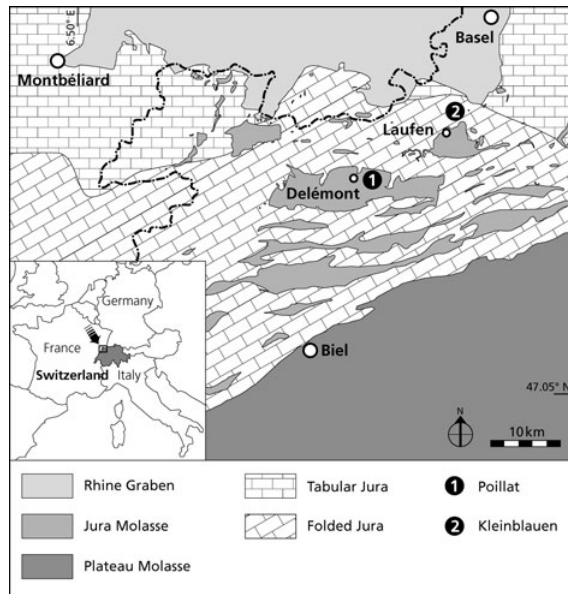


Figure 1. Geographical and geological setting of the Early Oligocene mammal localities of Poillat (Delémont valley, Canton Jura) and Kleinblauen (Canton Baselland) in the north-central Jura Molasse (NW Switzerland).

We report here a recently discovered, well-preserved skull and associated fragment of a juvenile mandible attributed to a new small-sized representative of Rhinocerotinae very close to *P. albigense*, *Molassitherium delemontense* gen. et sp. nov., from Poillat, a new Early Oligocene vertebrate locality within the Delémont valley (Canton Jura, NW Switzerland; Fig. 1). We include this sample as a terminal taxon in a cladistic analysis in order to establish its phylogenetic relationships, notably with other European Oligocene and Miocene rhinocerotids.

Material and methods

Material

The referred type material is stored in collection PAL A16 of the Natural History Museum of Canton Jura in Porrentruy, Switzerland (Musée jurassien des sciences naturelles). Large mammal remains were quarried in 2007 at Poillat in the Delémont valley (Canton Jura, NW Switzerland), during construction of motorway A16 (Transjurane) and small mammal teeth were discovered by screening washing the deposits from the same fossiliferous level (*c.* 350 kg).

The additional referred specimens of this study include dental remains from Offenheim (Germany), Kleinblauen (Switzerland) and Monclar-de-Quercy (France), attributed by Uhlig (1999) and Becker (2009) to *Epiaceratherium* aff. *magnum*, and also specimens from Habach 5, attributed by Göhlich (1992) to *Epiaceratherium* sp.

and by Uhlig (1999) to cf. *Epiaceratherium* sp. The specimens from Kleinblauen and from Monclar-de-Quercy have been reviewed based on the direct observations of the specimens housed in the Naturhistorisches Museum Basel (Switzerland) and the Muséum d'Histoire naturelle de Toulouse (France), respectively. Data on specimens from Offenheim (stored in the Hessischen Landesmuseum, Darmstadt, Germany) and Habach 5 (stored in the Bayerische Staatssammlung für Paläontologie und Historische Geologie, Munich, Germany) are based on the work of Uhlig (1999).

Stratigraphical context

The mammal remains from Poillat were trapped in Rupelian sandy deposits corresponding to the transition between the brackish lower part and the continental upper part of the 'Molasse alsacienne' (USM: Lower Freshwater Molasse). The general stratigraphical context of this Jura Molasse Formation (termed NW Swiss Molasse Basin) was described in previous works (Picot. *et al.* 2008; Becker 2009). The succession consists of a lithofacies assemblage (tabular sandy beds with sigmoidal or planar cross-stratifications, erosional sandy beds with low angle trough cross-stratifications or tough cross-stratifications, massive fines) typical of a coastal to alluvial floodplain controlled by a mouth complex of distributary channels, interdistributary bays and tidal bars, and by sandy channels and muddy floodplains. The new specimens reported in this paper originate from a sandy mud pebble channel.

The biochronological framework (Fig. 2) is based on the European Land Mammal Ages (ELMA) defined by the succession of European mammal reference levels (MP; Schmidt-Kittler *et al.* 1987) and the Palaeogene geological time scale (Luterbacher *et al.* 2004). The lithostratigraphical correlations follow the interpretation of Becker (2009). At the European scale, based on the biostratigraphy of the localities Kleinblauen (Switzerland, 'late MP22'; Becker 2009), Offenheim (Germany, MP23; Uhlig 1999), Habach 5 (Germany, MP25; Uhlig 1999) and Monclar-de-Quercy (France, MP25; Muratet *et al.* 1992), the stratigraphical range of *Molassitherium delemontense* gen. et sp. nov. corresponds to the 'late MP22'–MP25 interval (late Early–early Late Oligocene).

The rodent assemblage found in association with the rhinocerotid remains implies a late Early Oligocene age ('early MP24'; Online Supplementary Material). It includes the Theridomyidae *Blainvillimys helmeri* Vianey-Liaud, 1972, *Blainvillimys* aff. *heimersheimensis* Bahlo, 1975 and *Protechimys truci/lebratierensis* Hugueney, 1994/Vianey-Liaud, 1998, the Cricetidae *Paracricetodon dehmi* Hrubesch, 1957, *Pseudocricetodon* cf. *montalbaniensis* Thaler, 1969 and *Eucricetodon* cf. *huberi* (Schaub, 1925), as well as the glirid *Schizoglyiravus* cf. *tenuis* (Bahlo, 1975). The corresponding age for Poillat is around

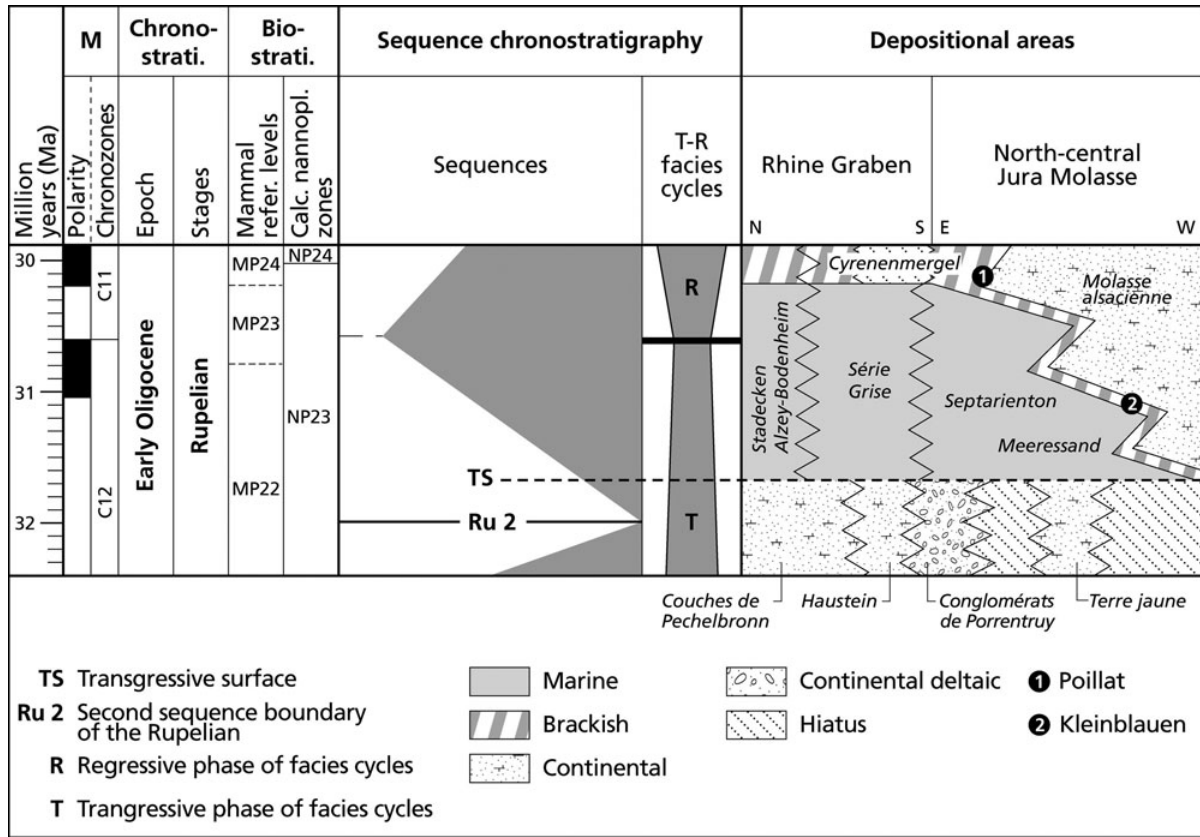


Figure 2. Lithostratigraphical correlation chart for the Early Oligocene of the Rhine Graben and north-central Jura Molasse (modified from Picot *et al.* 2008 and Becker 2009). Magnetostratigraphy (M), chronostratigraphy, mammal reference levels and calcareous nannoplankton zones follow Luterbacher *et al.* (2004) and sequence chronostratigraphy is after Hardenbol *et al.* (1998).

30–30.5 Ma, based on the calibrations of Legendre & Lévêque (1997) and Luterbacher *et al.* (2004).

Anatomical terminology and characters

Dental terminology follows Heissig (1969), Uhlig (1999) and Antoine (2002). Dental and osteological features described correspond basically to cladistic characters used and listed by Antoine (2002). Measurements were made according to Guérin (1980) and are given in mm.

Institutional abbreviations

AMNH: American Museum of Natural History, New York; **BSP:** Bayerische Staatssammlung für Paläontologie und Historische Geologie, Munich; **FSL:** Fondation Scientifique de Lyon; **HLM:** Hessischen Landesmuseum, Darmstadt; **UPM:** Université de Provence, Marseille Saint-Charles; **IPHEP:** Institut International de Paléoprimatologie, Paléontologie Humaine: Evolution et Paléoenvironnement, Poitiers; **MHNL:** Muséum d’Histoire naturelle de Lyon; **MHNT:** Muséum d’Histoire naturelle de Toulouse; **MJSN:** Musée jurassien des sciences naturelles, Porrentruy, Switzerland; **MNHN:** Muséum National d’Histoire Naturelle, Paris; **NHM:** Natural History

Museum, London; **NMB:** Naturhistorisches Museum Basel; **Rhinopolis:** Musée Rhinopolis, Gannat, France; **UCBL:** Université Claude-Bernard Lyon-Villeurbanne 1, France.

Anatomical abbreviations

I/i: upper/lower incisor; **C/c:** upper/lower canine; **P/p:** upper/lower premolar; **M/m:** upper/lower molar; **D/d:** upper/lower deciduous tooth; **ant:** anterior; **post:** posterior; **prox:** proximal; **dist:** distal; **l:** left; **r:** right; **H:** height; **L:** length; **W:** width.

Phylogenetic relationships

The dataset (character list, character states) derives from that of Antoine (2002, 2003) and Antoine *et al.* (2003b, 2010). It was reduced to 214 morphological characters (36 cranial, eight mandibular, 85 dental and 85 postcranial), as 68 characters from the original matrices were phylogenetically uninformative for the present taxonomic sample and therefore were removed prior to the analysis. The character listing and the data matrix can be found in Appendices 1 and 2.

Character coding sources, through direct observation and/or the literature, are given in Online Supplementary Material. Thirty terminal taxa were included in the phylogenetic analysis. Three terminals were selected as outgroups: the extant tapirid *Tapirus terrestris* Linnaeus, 1758, the Eocene hyrachyid rhinocerotoid *Hyrachyus eximius* Leidy, 1871 and the Eocene stem rhinocerotid *Trigonias osborni* (Lucas, 1900) from North America.

The in-group *sensu lato* consists of both taxa of interest (in-group *sensu stricto*) and selected terminals forming a 'branching group', *sensu* Antoine (2002) and Orliac *et al.* (2010). The in-group *sensu stricto* includes the earliest European rhinocerotid *Ronzotherium filholi* (Osborn, 1900) (from the earliest Oligocene of Europe) and an exhaustive specific sampling for *Pleuroceros* Roger, 1898 (with *P. pleuroceros* (Duvernoy, 1853) and *P. blanfordi* (Lydekker, 1884) from the Early Miocene of Europe and Pakistan, respectively), *Epiaceratherium* Abel, 1910 (with *E. bolcense* Abel, 1910 and *E. magnum* Uhlig, 1999, from the Early Oligocene of Western Europe), and *Mesaceratherium* Heissig, 1969 (with *M. paulhiacense* (Richard, 1937) and *M. gaimersheimense* Heissig, 1969, from around the Oligocene–Miocene transition in Europe, as well as *M. welcommi* Antoine & Downing in Antoine *et al.*, 2010, from the Early Miocene of Pakistan). The type species of *Protaceratherium* Abel, 1910, *Protaceratherium minutum* (Cuvier, 1822), from the Early Miocene of Western Europe, and *P. albigense* (Roman, 1912), from the 'middle' Oligocene of Europe, were also considered in the analysis in order to test the monophyly of the concerned genus, recently challenged in the phylogeny proposed by Antoine *et al.* (2010).

The branching group includes (1) type species or well-represented species of type genera of suprageneric groups recognized within Rhinocerotidae; and (2) early representatives of these suprageneric groups, in order to branch the taxa of interest within Rhinocerotidae, to define their generic and suprageneric affinities, and to avoid long-branch attraction artefacts due to parallelism (e.g. late representatives of Elasmotheriinae versus Rhinocerotinae; Antoine 2002). The present branching group comprises well-known Elasmotheriinae (early Elasmotheriina: *Hispanotherium beonense* (Antoine, 1997) and *Bugtirhinus praecursor* Antoine & Welcomme, 2000, from the Early Miocene of Europe and Pakistan, respectively; Menoceratina: *Menoceras arikareense* (Barbour, 1906), from the Early Miocene of North America; 'diceratheres': *Diceratherium armatum* Marsh, 1875 and *Subhyracodon occidentalis* (Leidy, 1851), from the Oligocene of North America) and Rhinocerotinae (Rhinocerotina: *Rhinoceros unicornis* Linnaeus, 1758, *R. sondaicus* Desmarest, 1822, *Diceros bicornis* (Linnaeus, 1758) and *Dicerorhinus sumatrensis* (Fischer Von Waldheim, 1814) [recent], and *Lartetotherium sansaniense* (Lartet, 1837), from the Miocene of Europe; Teleoceratina: *Teleoceras fossiger* (Cope, 1878),

from the late Miocene of North America, and *Prosantorhinus douvillei* (Osborn, 1900), from the late Early Miocene of Europe; Aceratheriini: *Aceratherium incisivum* Kaup, 1832, *Alicornops simorreense* (Lartet, 1851) and *Hoploaceratherium tetradactylum* (Lartet, 1851), from the middle and/or late Miocene of Europe; the hornless rhino *Plesiaceratherium mirallesi* (Crusafont *et al.*, 1955), from the late Early Miocene of Europe).

Systematic palaeontology

Order Perissodactyla Owen, 1848

Superfamily Rhinoceroidea Gray, 1821

Family Rhinocerotidae Gray, 1821

Subfamily Rhinocerotinae Gray, 1821

Unnamed clade

Molassitherium Becker & Antoine gen. nov.

Type species. *Acerotherium albigense* Roman, 1912 (including *Diceratherium kuntneri* Spillmann, 1969, p. 217, figs 16–18).

Other species. *Molassitherium delemontense* Becker & Antoine sp. nov.

Diagnosis. Small Rhinocerotinae characterized by possessing an occipital side of the skull inclined backward, short nasal bones, a forked occipital crest, by lacking any crochet on upper molars and by having a mesostyle on M2.

Differs from *Epiaceratherium* by having a narrow post-fossette on P2–4, a protocone always constricted on upper molars, a posterior part of the ectoloph concave on M1–2 and by lacking any metacone fold on M1–2. Further differs from *Epiaceratherium bolcense* by having a developed nuchal tubercle and a posterior margin of the pterygoid nearly horizontal, and also by lacking any metaloph constriction on P2–4 and any antecrochet on upper molars. Differs from *Epiaceratherium magnum* by lacking any cement on permanent cheek teeth, the protocone constriction on P3–4 and the crista on upper molars. Differs from *Mesaceratherium* by having a posterior groove on the ectometaloph of M3. Differs from *Pleuroceros* by lacking any crochet on P2–4 and by having a lingual cingulum always present on upper molars and a posterior groove on the ectometaloph of M3. Differs from *Protaceratherium minutum* by showing a developed nuchal tubercle, a labial cingulum usually or always present on upper premolars, a protoloph joined to the ectoloph on P2, an antecrochet always present on upper molars, a long metaloph on M1–2, a mesostyle on M2, a constricted protocone on M3 and a posterior groove on the ectometaloph of M3, as well as by lacking any crochet on upper premolars and any metacone fold on M1–2.

Derivation of name. From 'molasse', French, English and German word for fine detrital sedimentary rocks

archetypical of Alpine and Pyrenean piedmont Tertiary deposits which yielded most of the hypodigm of the included species, and ‘therium’, Greek for beast, a suffix widely used for rhinocerotids.

Occurrence. Early to early Late Oligocene (‘late MP22’–28; Rupelian–early Chattian), Europe and the Balkans (Turkish Thrace; Saraç 2003).

Molassitherium delemontense Becker & Antoine sp. nov.
(Figs 3–5)

1992 *Epiaceratherium* sp. Göhlich: 81.

1992 *Protaceratherium albigense* Muratet *et al.*: 1113.

1999 *Epiaceratherium* aff. *magnum* Uhlig: 88, fig. 61, pl. 2/21.

1999 cf. *Epiaceratherium* sp. Uhlig: 122, fig. 81.

2009 *Epiaceratherium* aff. *magnum* Becker: 493, fig. 4f.

Diagnosis. Early species of the genus, differing from the type species (*M. albigense*) by having nasals with a forked tip in dorsal view, a labial cingulum usually present and a transverse metaloph on upper premolars, a lingual bridge and a hypocone stronger than the protocone on P2, a lingual wall on P3–4, a labial cingulum usually absent on upper molars, a long metastyle on M1–2, somewhat distinct ectoloph and metaloph on M3, and also by lacking any constricted metaconid and any protoconid fold on lower milk teeth.

Derivation of name. After Delémont (Canton Jura, NW Switzerland), the name of the district where the locality of Poillat is situated.

Type material. Holotype: adult skull with left and right P1–M3, lacking the basioccipital, the nasal tip, the premaxilla as well as the anterior dentition (MJSN POI007–245). Paratype: juvenile mandible fragment with broken left d3–4 (MJSN POI007–268).

Type horizon. Sandy bed from the top of the brackish lower part of the *Molasse alsacienne* Formation of the USM (Lower Freshwater Molasse), European mammal reference level MP24.

Type locality. Poillat, eastern bank of the Birse River, near Courrendlin, Delémont district, Canton Jura, NW Switzerland.

Additional referred material. Toothrow with left P3–M1 (NMB KB7/1-7/3) from Kleinblauen (Switzerland, ‘late MP22’; Becker 2009, p. 493, fig. 4f); toothrow with right M2–M3 (HLM Din1477), toothrow with left P2–P3 (HLM Din2327), toothrow with right P2–P3 (HLM Din1478), toothrow with left p2–p3 (HLM Din1450), toothrow with left m1–m3 (HLM Din2326), and left p4 (HLM Din1454) from Offenheim (Germany, MP23; Uhlig 1999, p. 88, fig. 61); right M2, left M3, right P3 (fragment), left P4 (fragment) (BSP 1977 XXVI 112–115) from Habach 5

(Germany, MP25; Göhlich 1992, p. 81; Uhlig 1999, p. 122, fig. 81); left M2 (fragment) (MHNT), right M3 (MHNT; cast BSP 1968 XIV 81 illustrated in Uhlig 1999, p. 91, pl. II/21) from Monclar-de-Quercy (France, MP25; Muratet *et al.* 1992, p. 1113).

Occurrence. Late Early Oligocene (‘late MP22’–MP25) of Western Europe (Germany, Switzerland and France).

Description

Skull. The well-preserved skull (MJSN POI007–245) belongs to a small-sized adult rhinoceros. It lacks the basioccipital, the nasal tip, as well as the premaxilla and the anterior dentition. The nasal bones have a forked tip in dorsal view but they do not display any lateral apophysis on their ventral edge in lateral view. The foramen infraorbitalis is above P3. The nasal notch is wide, deep and U-shaped, reaching the P3/4 limit. The anterior border of the orbit is above the anterior part of M2. There is neither septum ossification nor lateral projection of the orbit. The nasal/lacrimal suture is long. The jugal/squamosal suture is smooth. A weak lacrimal process is present and the postorbital process is absent. The anterior base of the zygomatic process of the maxilla is low, beginning less than one centimetre above the neck of M2. The zygomatic arch is high (nearly reaching the level of the cranial roof) and fairly developed. It forms a thin sigmoid strip, without postorbital process. The dorsal profile of the skull is flat. The sphenorbitale and rotundum foramina are not observable and the area between the temporal and nuchal crests is depressed. The external auditory pseudomeatus is open ventrally. The occipital side is inclined up and backwards with a very acute angle and a developed nuchal tubercle. The posterior margin of the pterygoid is nearly horizontal. The nasal bones are totally separate from one another by a shallow median groove. They are straight, short and triangular, and lacking any vascular print or domed structure indicating the presence of nasal horn(s), although the tip is lacking. Also, despite the lack of the premaxilla, it can be assumed that the skull was dolicocephalic (maximum zygomatic width/nasal–occipital length ratio < 0.50). There is no evidence for any frontal horn. The frontal bones are wide with respect to the zygomatic bones (zygomatic width/frontal width ratio = 1.34). The fronto-parietal crests are sharp and salient. They are joined (constricted) in their posterior halves, only separated by a strongly constricted groove (*c.* 2 mm wide), and then slightly separated, forming a weak dome just prior the occipital crest. The latter is strongly concave, deeply forked and narrow (*c.* 106 mm).

In palatine view, the anterior end of the zygomatic process of the maxilla progressively diverges from the curvature of the tooth row and distally becomes parallel to the skull axis. The palate is quite wide. The palatine fossa reaches mid-length of the M2 and the vomer is acute. The glenoid cavity (fossa mandibularis) is flat and forms a

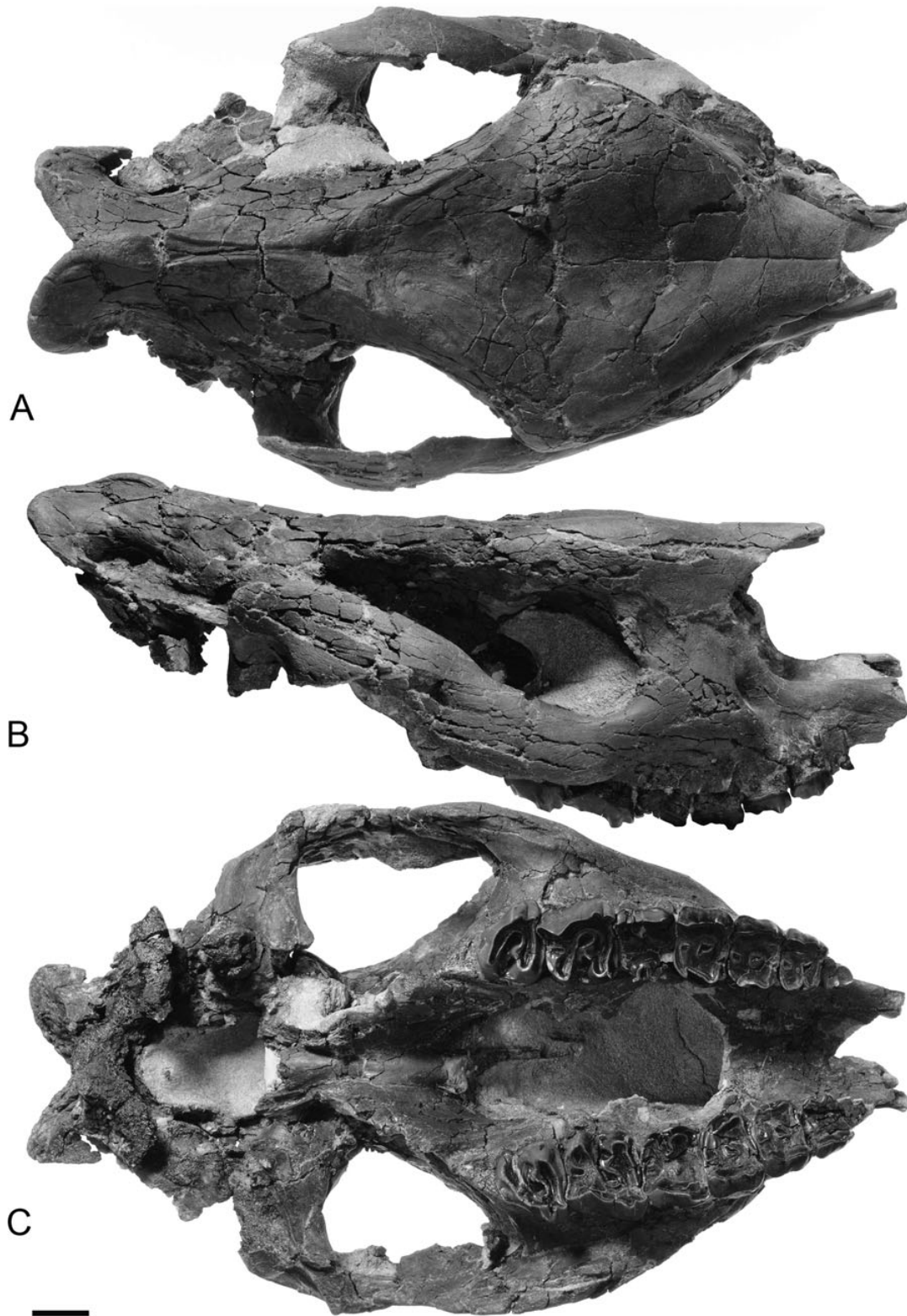


Figure 3. *Molassitherium delemontense* gen. et sp. nov. from the late Early Oligocene of Poillat (Delémont valley, Canton Jura, NW Switzerland), MJSN POI007–245 (holotype). Skull in **A**, dorsal; **B**, lateral; and **C**, ventral views. Scale bar equals 30 mm.

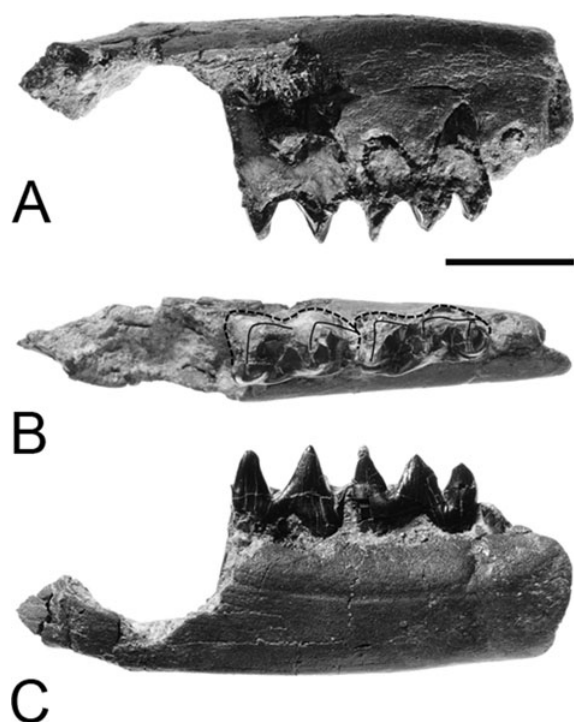


Figure 4. *Molassitherium delemontense* gen. et sp. nov. from the late Early Oligocene of Poillat (Delémont valley, Canton Jura, NW Switzerland), MJSN POI007–268 (paratype). Fragment of a left juvenile mandible with broken d3–4, in **A**, lateral; **B**, occlusal; and **C**, medial views. Scale bar equals 30 mm.

smooth semi-cylinder in lateral view. The articular tubercle of the squamosal is high with a concave transverse profile. The foramen postglenoideum is distant from the postglenoid process. The latter is robust and its articular surface is angular in cross-section. The post-tympanic and paraoccipital processes are well developed. There is no posterior groove of the processus zygomatic.

Mandible. The corpus mandibulae of the fragmentary juvenile specimen MJSN POI007–268 bears a lingual groove and seems to have a straight ventral profile.

Dentition. Only the distal part of the diastema (3 cm long) is preserved on skull MJSN POI007–245; it shows neither canine nor incisor alveolus. The premolar series is long when compared to the molar series (LP3–4/LM1–3 ratio = 0.54). The P1–3 and M1 of skull MJSN POI007–245 are much worn, precluding detailed observation. The upper cheek teeth (except P1) are characterized by an internal wall strongly inclined labially. The dental structures are simple and there are no secondary enamel folds or cement on the crowns. The enamel is thin and wrinkled. The crowns are low (brachyodont teeth) and the roots are long, distinct and divergent. The crochet and the medifossette are always

absent and the postfossette narrow. The paracone fold is constant and thick on P2–M3, vanishing before the neck and thus not visible on very worn teeth. The parastyle is sagittally oriented, more developed on upper molars than on premolars. The metacone fold is weakly developed on P2–4, absent on M1–2 and fairly distinct on M3. The mesostyle is smooth on P2–4 and very faint on M1–2. There is a very thin continuous labial cingulum on P2–4 of MJSN POI007–245, running all along the cervix. This labial cingulum tends to be reduced on M1–2 and it is restricted to a strong distolabial spur on M3. It is reduced in specimens from Offenheim, Grafenmühle 11 and Monclarde-Quercy; by contrast, it is rather developed in specimens from Kleinblauen and Habach 5. The lingual cingulum is always present and strong: it is continuous on P2 (weaker under the protocone and hypocone), continuous to reduced under the protocone on P3–4 and reduced under the protocone and the hypocone on M1–3 (restricted to an enamel bridge at the lingual opening of the median valley).

P1 is two-rooted and trapezoidal in occlusal view (mesially tapered and approximately the same length as distal width), with a rectilinear lingual side and a rounded mesiolabial side. It is much narrower than P2 and bears a lingual groove on the protoloph and a thin lingual cingulum in its mesial half. The protocone and the hypocone on P2 are joined by a lingual bridge (semi-molariform pattern *sensu* Heissig 1969). The protocone is less developed than the hypocone. The protoloph is thin but continuous and widely connected with the ectoloph, and the metaloph is transverse. P3–4 display a lingual wall marked by a smooth vertical groove (P3 being semi- to submolariform, P4 sub- to premolariform *sensu* Heissig 1969) and taper distally, especially P4, with a transverse metaloph shorter than the protoloph. Additionally, P3 and P4 bear a smooth crista and a weak anterior groove on the protocone (particularly visible on P3–4 NMB KB7/1-7/2 from Kleinblauen) and the P3 NMB KB7/1 from Kleinblauen possesses an antecrochet. There is no pseudometaloph on P3 (*sensu* Antoine 2002).

The upper molars have a median valley with a labial pit. M2 is larger than M1. Both the metastyle and the metaloph are long and the posterior part of the ectoloph is concave on M1–2 (no metacone fold). The metaloph is constricted on M1–2: there is a mesiolingual groove on the hypocone of M1–2. There is a strong constriction of the protocone and a strongly developed antecrochet on M1–3. The postfossette is deeper than the distal cingulum. M3 has an ectometaloph (resulting from the fusion of the ectoloph and the metaloph), a quadrangular occlusal outline, a strong bump-shaped posterior cingulum (metastyle artefact), a faint metacone fold and a smooth posterior groove on the lower part of the crown. The protoloph of M3 is transverse and straight and the protocone is trefoil-shaped.

The lower milk teeth do not exhibit any constriction of the metaconid. The d3 shows a strong protoconid fold and a forked paralophid. The mesial branch of the latter seems

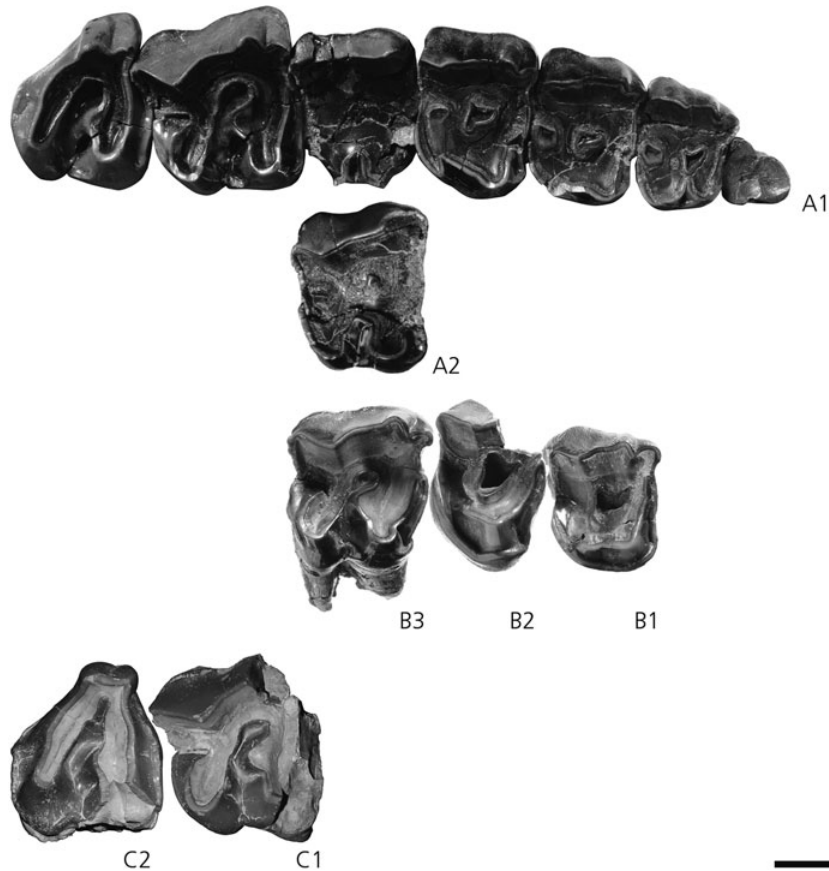


Figure 5. *Molassitherium delemontense* gen. et sp. nov. A1–2, right upper tooth row and left M1 (reversed) of the skull MJSN POI007–245 (holotype) from the late Early Oligocene of Poillat (Delémont valley, Canton Jura, NW Switzerland), in occlusal view. B1–3, left (reversed) P3–M1 NMB KB7/1-7/3 from Kleinblauen (Canton Baselland, NW Switzerland), in occlusal view. C1–2, left (reversed) M2 MHNT, right M3 MHNT from Monclar-de-Quercy (France), in occlusal view. Scale bar equals 30 mm.

very short, whereas a well-developed oblique anterior crest characterizes its lingual branch. There is no lingual groove on the entoconid of the d3. The d4 exhibits a constriction of the entoconid on the upper part of the crown.

Remarks. Numerous cranial and dental features, such as a lozenge-like dorsal outline of the skull, the occipital side tilted backwards, the presence of an antecrochet and of a constricted protocone on the upper molars (Antoine *et al.* 2003b, 2010) point to Rhinocerotidae and preclude assignment of these specimens to Hyracodontidae (*Eggysodon*) and Amynodontidae (*Cadurcotherium*), two rhinocerotoid families which are also documented in the Oligocene of Europe. Five rhinocerotid genera are known to occur in the European Oligocene (Uhlig 1999; Antoine *et al.* 2003a, 2006; Ménouret & Guérin 2009): *Epiaceratherium* Abel, 1910 (Early Oligocene), *Ronzotherium* Aymard, 1854 (Oligocene), *Protaceratherium* Abel, 1910 (Roman 1912) (late Early Oligocene to Early Miocene), *Mesaceratherium*

Heissig, 1969 (Late Oligocene to Early Miocene) and *Diaceratherium* Dietrich, 1931 (early Late Oligocene to Early Miocene). *Ronzotherium* differs in its larger dimensions, concave dorsal profile of the skull, high anterior base of the zygomatic process distally widely diverging from the curvature of the tooth row, stronger cingula on upper cheek teeth and straight posterior part of the ectoloph on M2 (Heissig 1969; Brunet 1979; Becker 2009). *Mesaceratherium* and *Diaceratherium* are of larger size and differ by their more advanced molarization of the upper premolars (Heissig 1969; de Bonis 1973; Becker *et al.* 2009; Ménouret & Guérin, 2009). Moreover, the occipital crest of *Diaceratherium* skulls can be sometimes concave but is never deeply forked (Becker *et al.* 2009) and *Mesaceratherium* displays no posterior groove on the ectometaloph on M3 (Antoine *et al.* 2010). Also, the referred upper cheek teeth differ from those of *Protaceratherium minutum* by showing a labial cingulum present on the upper premolars, no crochet on the upper premolars, a protoloph joined to the

ectoloph on P2, an antecrochet always present on the upper molars, no metacone fold but a long metaloph on M1–2, a mesostyle on M2, a constricted protocone on M3 and a posterior groove on the ectometaloph of M3. Additionally, the skull from Poillat displays both a narrow zygomatic arch with a low anterior base of the zygomatic process distally becoming parallel to the skull axis and a wide and deep U-shaped nasal notch, which are reminiscent of the North American early diverging rhinocerotid *Trigonias* Lucas, 1900. However, the latter differs in its concave dorsal profile, elevation of the occipital crest, a somewhat concave occipital crest and a more advanced molarization of the upper premolars (Wood 1932; Prothero 2005).

The referred specimens share with *Epiaceratherium* the following features: P2–M3 with convergent lingual and labial walls, upper premolars with a metacone fold always developed and a lingual cingulum strongly developed, upper molars with a strong paracone fold and a restricted lingual cingulum at the lingual opening of the median valley, and an M2 larger than M1 (Uhlig 1999). However, *Epiaceratherium* displays a wide postfossette on P2–4 and a metacone fold and the posterior part of the ectoloph straight on M1–2. *Epiaceratherium bolcense* differs by being smaller, by having a proportionally narrower nasal notch, a posterior margin of the pterygoid nearly horizontal, less molarized upper premolars, the presence of a metaconid constriction on lower milk teeth, and also by lacking any metaloph constriction on P2–4, and any protocone constriction and antecrochet on upper molars. On the other hand, the referred specimens are of similar size and have numerous similarities with those of *E. magnum*, such as a strong lingual cingulum elevated under the main cusps and a distinct mesostyle on P2–4 (Uhlig 1999; Becker 2009). However, the absence of cement on adult cheek teeth, the slightly more advanced molarization of the upper premolars, the more developed paracone fold on P2–M3, the anterior protocone groove and the lingual wall marked by a smooth groove on P3–4, the absence of crista on upper molars, the constricted protocone, the strongly marked antecrochet the concavity of the posterior part of the ectoloph on M1–2, the quadrangular M3 with distinct ectoloph and metaloph, a metastyle artefact, a faint metacone fold, a constricted protocone and a smooth posterior groove on the lower part of the crown, as well as a protoconid fold on d3, make them distinct from *E. magnum*. On the other hand, most of these characters are also described on the upper cheek teeth specimens from Offenheim (Germany), Kleinblauen (Switzerland) and Monclar-de-Quercy (France) attributed to *E. aff. magnum* by Uhlig (1999) and Becker (2009), and partly on the specimens from Habach 5 (Germany) attributed to cf. *Epiaceratherium* sp. by Uhlig (1999). Only the P2 from Weissenburg 16 (Germany, MP21?; Uhlig 1999) attributed by Uhlig (1999) to cf. *Epiaceratherium* sp. differs in being more primitive (submolariform) and smaller, and by having

a straight ectoloph profile. This specimen, despite the presence of a labial cingulum, seems to be referable to *E. bolcense* (Dal Piaz 1930; Uhlig, 1999).

Finally, most of the characters observed on all referred specimens, such as an occipital side of the skull inclined up and backwards, a posterior margin of the pterygoid nearly horizontal, short nasal bones, a forked occipital crest, an acute vomer, a labial cingulum usually present on the upper premolars, as well as a strongly marked antecrochet, a crochet always absent, a constriction of the protocone present, and a posterior part of the ectoloph concave on upper molars, a weakly developed mesostyle on M2, and a quadrangular M3, point to strong similarities with *Protaceratherium albigense* (Spillmann 1969; Lihoreau *et al.* 2009). However, the specimens from Poillat and the additional referred material can be distinguished from the latter by having smaller dimensions (especially the M2), a high anterior base of the zygomatic process distally widely diverging, a narrower nasal notch and no labial pit of the median valley on the upper molars (Roman 1912; Hugueneu & Guérin 1981; Uhlig 1999; Lihoreau *et al.* 2009), as well as additional features discussed in the phylogenetic analysis section below.

Regarding the lower cheek teeth from Offenheim, attributed by Uhlig (1999) to *E. aff. magnum*, they display a trigonid with an acute dihedral and a posterior valley lingually open on p2 similar to *P. albigense* but differ in being larger and lacking any labial and lingual cingula. As described above, the smaller dimensions and the reduction of the cingula can also be observed on the upper cheek teeth to distinguish *P. albigense* from the referred material. The association of these lower cheek teeth from Offenheim with the upper ones as proposed by Uhlig (1999) is probably correct, leading us to list them in the additional material referred to *Molassitherium delemontense* gen. et sp. nov. However, as the specimens are scarce and their specific assignment is insufficiently constrained, we have excluded them from the phylogenetic analysis.

As a result, we favour assignment of the specimens from Poillat and the additional referred material from Germany, Switzerland and France, attributed to *Epiaceratherium aff. magnum* and to cf. *Epiaceratherium* sp. by Uhlig (1999) and Becker (2009), to *Molassitherium delemontense* gen. et sp. nov. This new taxon is considered to be the sister species of *M. albigense* comb. nov. More features are discussed in the phylogenetic analysis section (see below), including differences with the species of *Epiaceratherium* and *Protaceratherium* to which specimens of *Molassitherium delemontense* gen. et sp. nov. were formerly referred. (See Tables 1 and 2 for comparisons of cranial dental measurements).

Phylogenetic relationships

Only one most parsimonious tree (1117 steps; Consistency Index (CI) = 0.26; Retention Index (RI) = 0.48) was

Table 1. Cranial dimensions (in mm) of *Molassitherium delemontense* gen. et sp. nov. from the late Early Oligocene of Poillat (Delémont valley, Canton Jura, NW Switzerland), MJSN POI007–245 (holotype), and from other localities, and of *M. albigense*, *Epiaceratherium bolcense* and *Trigonias osborni* from their main localities.

Measurements (mm)	<i>Trigonias osborni</i> Prothero 2005	<i>Epiaceratherium bolcense</i> Monteviale Dal Piaz 1930	<i>Molassitherium delemontense</i> gen. et sp. nov. Poillat; MJSN POI007-245 this study	<i>Molassitherium albigense</i> comb. nov. Moissac; IPHEP MOI3.002 Lihoreau <i>et al.</i> 2009
Length occipital crest/tip of nasal			>415	(375)
Length occipital crest/tip of premaxilla		(455)	>466	450
Length occipital crest/caudal end of M3			287	210
Length end of M3/tip of premaxilla			>214	240
Length occipital crest/front of orbit			335	(247)
Length of nasal notch		89	>56	(85)
Minimum orbit width			89	
Length nasal notch/front of orbit			70	
Length tip of nasal/front of orbit			>141	
Minimum width of frontoparietal crest			10	
Maximum frontal width			(199)	(170)
Maximum zygomatic width	232 (n = 16)	260	260	(243)
Maximum nasal notch width			(73)	
Occipital crest width	121 (n = 16)		106	(est. 90)
Skull height (above P1)			119	
Skull height (above P4/M1)			144	
Skull height (above M3)			128	
Palate width (at P1 level)			62	43
Palate width (at P4/M1 level)			(71)	56
Palate width (at M3 level)		(80)	77	59
Length P1-M3		165.2 (n = 4)	181.5/(183.0)	171.0/171.0
Length P1-4		80.7 (n = 5)	88.0/(86.0)	87.0/87.0
Length P3-4		46.7 (n = 6)	53.0/(54.0)	47.0/47.0
Length M1-3	113 (n = 17)	86.5 (n = 5)	97.0/98.5	90.0/(88.0)
LP3-4/LM1-3		0.54	0.55	0.53

obtained by using the ‘mh*bb*’ command of Hennig86, 1.5 (Farris 1988) and the heuristic search of PAUP 4.0v10 (unweighted parsimony; branchswapping TBR, 1000 replications with random taxa addition, 100 tree-holds by replication; Swofford, 2002). This tree is shown in Fig. 6. Branch support, assessed by calculating the Bremer indices (Bremer 1994), is indicated below the branches in Fig. 6 (italicized), while the number of unambiguous synapomorphies (detailed in Table 3) appears above the branches, both left of the corresponding node. Nodes discussed in the text are designated by a letter, right of each node in the same figure (Fig. 6).

Suprageneric relationships within Rhinocerotidae are consistent with other recent phylogenies, such as those proposed by Antoine *et al.* (2010; based on a similar taxonomic sample) and, to a lesser extent, Antoine (2002) and Antoine *et al.* (2003a). The early rhinocerotid *Trigonias osborni* is remote from other Rhinocerotidae (Fig. 6). A basal split within Rhinocerotidae coincides with the well-supported divergence of the Elasmotheriinae and Rhinocerotinae clades (Fig. 6, node A). Elasmotheriinae consist of [*Ronzotherium filholi* [*Subhyracodon occidentalis* [*Diceratherium armatum* [*Menoceras arikarensis*

[*Hispanotherium beonense*, *Bugtirhinus praecursor*]]]]], as in Antoine *et al.* (2010). All the corresponding nodes are well supported, with Bremer indices ≥ 4 , and the number of unambiguous synapomorphies comprised between 7 and 23 (Fig. 6).

Relationships within Rhinocerotinae are as follows: [*Epiaceratherium bolcense* [*Epiaceratherium magnum* [*Molassitherium* [*Mesaceratherium* [*Pleuroceros* [*Protaceratherium minutum* [*Plesiaceratherium mirallesi* [*Aceratheriini*, *Rhinocerotini*]]]]]]]]], as illustrated in Fig. 6 (node B). The only paraphyletic genus in the analysis is *Epiaceratherium*, with the earliest Oligocene *E. bolcense* being sister group to all other Rhinocerotinae (topology supported by seven synapomorphies, the less homoplastic of which are the presence of a constricted hypocone on M1 [RI = 0.50] and M2 [RI = 0.61] and a low trochanter major on the femur [RI = 0.50]) and the Early Oligocene *E. magnum* as the next offshoot (dichotomy supported by four less homoplastic unambiguous synapomorphies: labial cingulum usually absent [RI = 0.69] and antecrochet always present [RI = 0.69] on upper molars; protocone usually constricted on M1–2 [RI = 0.67] but usually unconstricted on M3 [RI = 0.54]). Node C coincides

Table 2. Dental measurements (in mm) of the upper cheek teeth of *Molassitherium delemontense* gen. et sp. nov. and of *M. albigenae*, *Epiacetherium magnum*, *Epiacetherium bolcense* and *Trigonias osborni*.

Taxa	Locality (housing institution)	Reference	Tooth	n	L	Mes. W	Dist. W	H			
<i>Trigonias osborni</i>		Prothero 2005	P2	6	24.0	27.0	—	—			
			P3	7	24.0	26.0	—	—			
			P4	10	26.0	39.0	—	—			
			M1	9	33.0	43.0	—	—			
			M2	9	39.0	48.0	—	—			
			M3	9	—	44.0	—	—			
			P1	6	17.7 [15.6-18.3]	—	14.4 [12.0-16.2]	—			
			P2	4	18.9 [18.0-19.5]	—	23.1 [22.2-24.4]	—			
			P3	6	22.3 [20.2-24.4]	27.8 [27.0-30.0]	—	—			
<i>Epiacetherium bocense</i>	Monteviale	Dal Piaz 1930	P4	6	24.4 [23.4-26.0]	32.7 [31.4-34.0]	—	—			
			M1	5	24.7 [27.8-32.6]	—	34.9 [34.2-35.4]	—			
			M2	5	32.7 [32.0-34.8]	—	37.1 [36.4-38.4]	—			
			M3	5	—	33.9 [31.8-37.0]	—	—			
			P1	18	18.5 [17.0-20.0]	13.9 [12.5-15.5]	—	—			
			P2	10	21.9 [18.5-23.0]	26.0 [23.0-29.0]	27.5 [24.0-30.0]	—			
			P3	5	19.6 [23.0-26.0]	34.1 [32.0-35.5]	32.4 [31.0-34.0]	—			
			P4	9	26.4 [25.0-27.5]	38.4 [35.0-40.5]	40.6 [32.0-37.0]	—			
			M1	8	32.6 [30.0-35.0]	38.0 [35.5-40.0]	35.7 [34.0-37.0]	—			
<i>Epiacetherium magnum</i>	Möhren 13 (BSP)	Uhlrig 1999	M2	1	36.0	40.0	35.5	(23.0)			
			M3	1	41.5	43.5	40.0	(27.0)			
			d3	8	35.8 [33.5-38.0]	42.1 [39.0-45.0]	39.0 [37.0-41.5]	—			
			d4	7	30.8 [29.0-32.0]	13.6 [13-14.0]	15.5 [14.0-17.0]	—			
			P1	1	28.4 [26.5-29.5]	16.9 [16.5-17.0]	18.4 [17.5-19.0]	—			
			P2	2	23.25 [23.5-23.0]	27.5 [27.0-28.0]	30.5 [31.0-30.0]	—			
			P3	2	26.0 [26.5-25.5]	35.0 [34.5-35.5]	34.5 [34.0-35.0]	—			
			P4	2	27.25 [27.0-27.5]	39.25 [39.5-40.0]	37.5 [36.5-38.5]	—			
			<i>Molassitherium delemontense</i> gen. et sp. nov.	Kleinblauen (NMB KB84) Möhren 13 (BSP) Kleinblauen (NMB KB83) Möhren 13 (BSP) Kleinblauen (NMB KB210) Möhren 13 (BSP) Poillat (MJSN POI007-245) Offenheim (BSP) Poillat (MJSN POI007-245) Kleinblauen (NMB KB7/3) Offenheim (BSP) Habach 5 (BSP) Poillat (MJSN POI007-245) Kleinblauen (NMB KB7/2) Offenheim (BSP)	Becker 2009 Uhlrig 1999 Becker 2009 Uhlrig 1999 Becker 2009 Uhlrig 1999 this study Uhlrig 1999 this study this study Uhlrig 1999 Uhlrig 1999 this study this study Uhlrig 1999	P1	1	31.0	43.5	—	—
						P2	2	22.0	29.0	29.0	—
P3	1	26.0				33.0	34.5	—			
P4	1	24.0 [24.0- —]				36.0 [— -36.0]	34.0 [— -34.0]	—			
P1	1	17.5				—	15.5	—			
P2	2	23.5				27.5	30.5	—			
P3	2	26.5				35.0	34.5	—			
P4	2	27.5				39.5	37.5	—			
P1	1	29.0				41.0	38.0	—			
P2	1	29.0				41.0	38.0	—			

(Continued on next page)

Table 2. (Continued)

Taxa	Locality (housing institution)	Reference	Tooth	n	L	Mes. W	Dist. W	H
	Poillat (MJSN POI007-245)	this study	M1	2	31.25 [30.0-32.5]	40.5 [40.5-40.5]	37.5 [37.5-37.5]	—
	Kleinblauen (NMB KB7/1)	this study		1	34.0	39.5	37.5	—
	Poillat (MJSN POI007-245)	this study	M2	2	39.75 [39.5-40.0]	44.5 [44.0-45.0]	39.75 [39.5-40.0]	—
	Offenheim (BSP)	Uhlig 1999		1	>32.0	43.0	(40.0)	—
	Habach 5 (BSP)	Uhlig 1999		1	>30.0	40.0	38.0	—
	Poillat (MJSN POI007-245)	this study	M3	2	33.5 [33.5-33.5]	41.5 [41.5-41.5]	—	—
	Offenheim (BSP)	Uhlig 1999		1	(36.0)	(45.0)	—	—
	Monclar de Quercy (MNHT)	this study		1	35.0	(44.0)	—	—
	Habach 5 (BSP)	Uhlig 1999		1	33.0	42.0	—	>26.0
	Poillat (MJSN POI007-268)	this study	d3	1	30.5	—	—	22.0
		this study	d4	1	27.5	—	—	18.5
	Moissac (IPHEP MOI3.002)	Lihoreau <i>et al.</i> 2009	P1	2	19.5 [19.0-20.0]	13.0 [12.5-13.5]	17.0 [15.5-16.5]	5.25 [5.0-5.5]
			P2	2	22.5 [22.5-22.5]	24.75 [24.5-25.0]	26.0 [26.0-26.0]	11.5 [11.0-12.0]
			P3	2	24.25 [24.0-24.5]	31.25 [31.0-31.5]	30.5 [30.5-30.5]	12.25 [12.0-12.5]
			P4	2	25.5 [25.5-25.5]	32.5 [32.0-33.0]	31.5 [30.5-31.5]	14.5 [14.0-15.0]
			M1	2	31.0	36.75 [36.0-37.5]	33.75 [33.5-34.0]	11.0 [11.0-11.0]
			M2	2	34.5	38.0 [38.0-38.0]	32.5 [32.5-32.5]	15.0 [14.5-15.5]
			M3	2	28.25 [28.0-28.5]	34.0 [33.5-34.5]	—	18.0 [17.5-18.5]

Molassitherium
albigense comb. nov.

Table 3. Distribution of unambiguous synapomorphies in the strict consensus tree illustrated in Fig. 6. Superscript numbers correspond to character states. Reversions are preceded by '-'. Nonhomoplastic synapomorphies (consistency index = retention index (RI) = 1) are bold-typed; weakly homoplastic apomorphies (RI ≥ 0.80) and unique reversals are underlined. Other characters are strongly homoplastic.

Node A: (Rhinocerotinae + Elasmotheriinae): 29¹, 67¹, -70¹, 76³, 82², 83¹, 90¹, 204¹
 Node B: (Rhinocerotinae): 61¹, 71¹, 94¹, 96¹, 156¹, 173¹, 200¹
 Node C: 53¹, -67⁰, 87³, 92¹, -108⁰, 113², 157¹
 Node D: (*Molassitherium delemontense* gen. et sp. nov., *Molassitherium albigense* comb. nov.): 12², 18¹, 24², -83⁰, 97¹
 Node E: -76², 83³, 101¹, 179¹, 188¹, -204⁰
 Node F: (*Mesaceratherium*): 165², 207¹
 Node G: 49¹, 62¹, 79², 117¹
 Node H: (*Pleuroceros*): 37², 66¹, 79³, -103¹, 109¹, 170¹, 171¹, 214¹
 Node I: 62², 74¹, -82², -123⁰, 151¹, 195¹, -197⁰, 199¹
 Node J: -4⁰, -12⁰, -96⁰, **99¹**, 104¹, 112¹, 121¹, **133¹**, 137¹, 141¹, 201²
 Node K: (Aceratheriini + Rhinocerotini): 34¹, 72¹, -92⁰, 138¹, 164¹, 165², 171¹
 Node L: (Aceratheriini): 25¹, 33¹, 44¹, 58¹, 64¹, 70², -74⁰, 84¹, 126¹
 Node M: (Rhinocerotini): 5¹, 8¹, 61³, 81³, 110¹, 149¹, -151⁰
 Node N: (Teleoceratina): 39¹, -51⁰, 63², 71¹, 79³, 97¹, 128³, **129¹**, 130¹, 136², 144², 147¹, 150¹, **168¹**, 169⁰, 178¹, 188², 193¹, 198¹, 199⁰, 207¹, 209¹, **212¹**
 Node O: (Rhinocerotina): 16¹, 19¹, 23², 30¹, -79⁰, -82⁰, -87², 108³, 114¹, 169², 199², 213¹

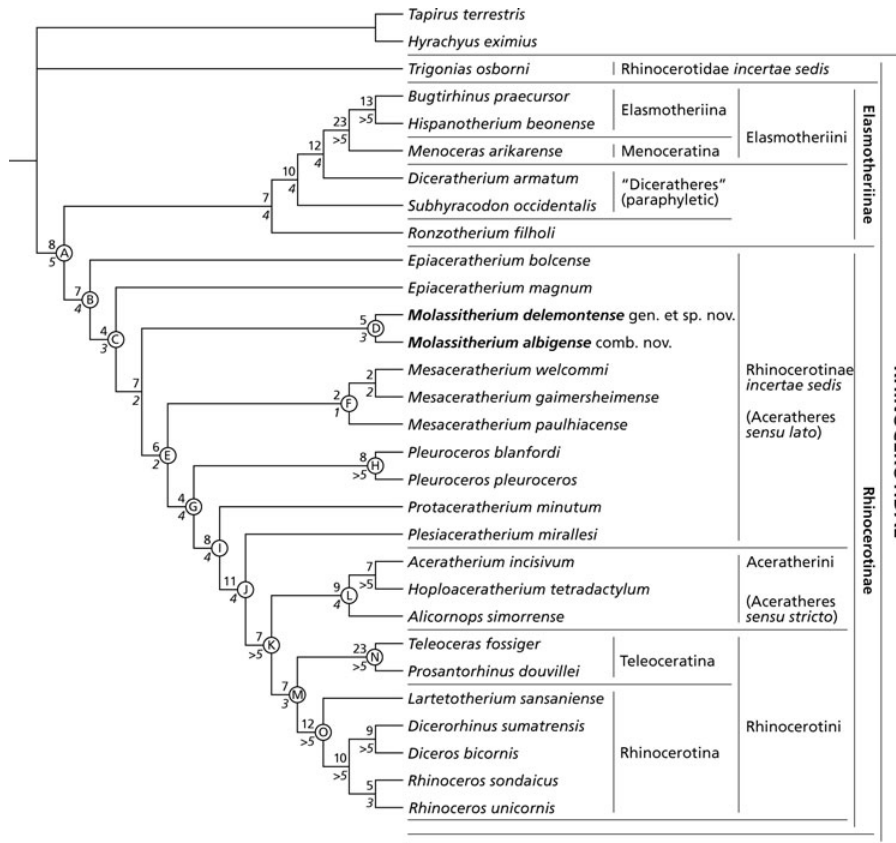


Figure 6. Most parsimonious tree (1117 steps; Consistency Index = 0.26; Retention Index = 0.48) obtained using Hennig86 1.5 (Farris 1988) and PAUP 4.0v10 (Swofford 2002), based on 214 morphological characters and performed on 30 rhinocerotid, rhinocerotoid and tapirid taxa, with *Tapirus terrestris*, *Hyrachyus eximius* and *Trigonias osborni* as outgroups. Suprageneric group names are based on current phylogenetic relationships and are consistent with those proposed by Antoine *et al.* (2010). Branch supports, assessed by calculating the Bremer Index (Bremer 1994), are indicated below the branches and italicized. The number of unambiguous synapomorphies for each node appears above the internal branches. The main nodes are designated by letters.

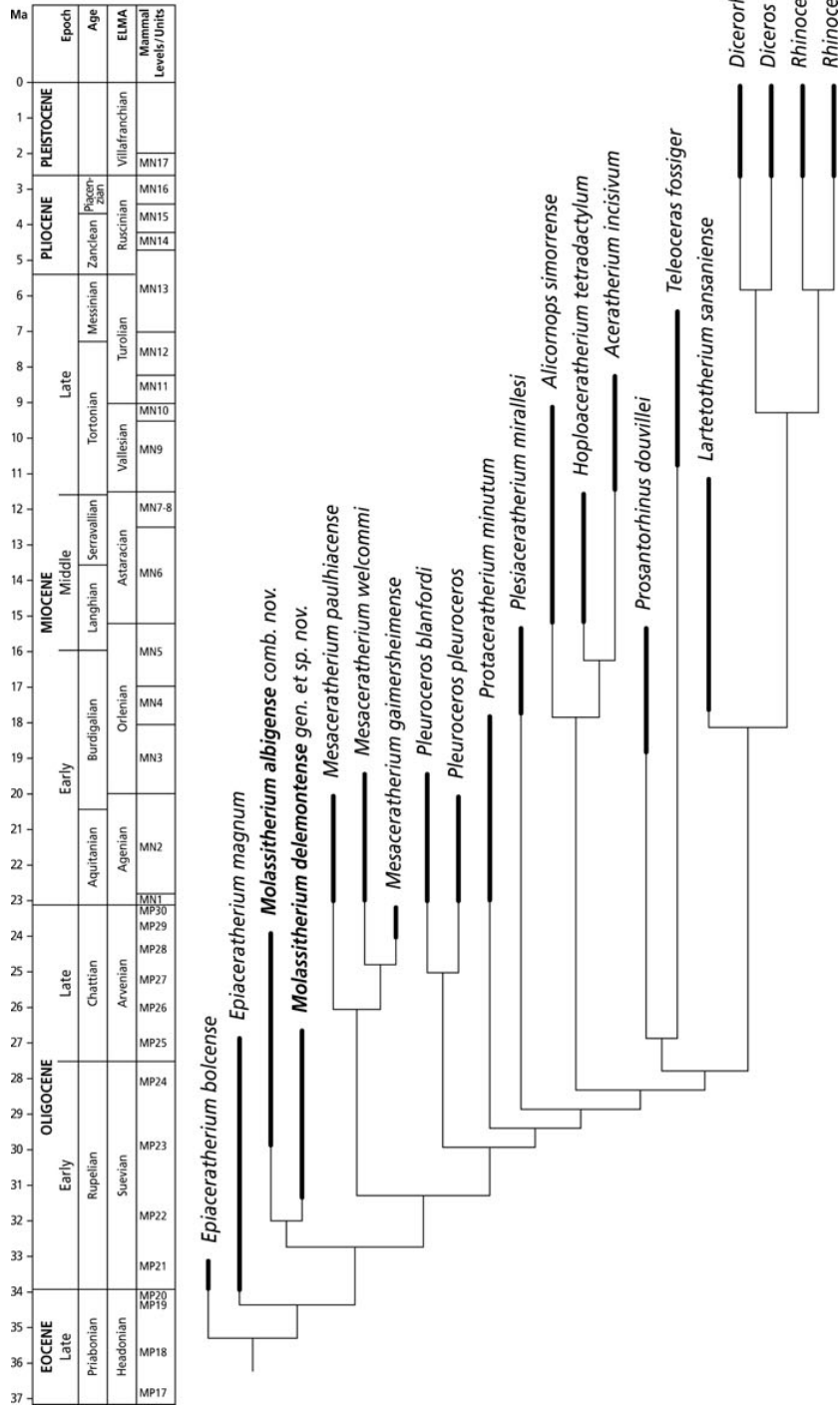


Figure 7. Biostratigraphically calibrated phylogeny of Rhinocerotinae focused on Oligocene taxa. Long branches (ghost lineages) are inferred by the absence in the current analysis of key early taxa referred either to *Plesiaceratherium*, *Teleoceras* or *Rhinocerotina*. Based on data from Heissig (1969, 1989, 1999), Antoine *et al.* (1997, 2000, 2003b, 2006, 2010, 2011), Uhlrig (1999), Antoine (2002, 2012), Becker (2009) and Lihoreau *et al.* (2009).

with the divergence of *Molassitherium* from more derived Rhinocerotinae (I3 absent [optimized; RI = 0.75]; wide postfossette on P2–4 [RI = 0.40]; protocone always constricted on M1–2 [RI = 0.67]; posterior part of the ectoloph concave on M1–2 [RI = 0.69]; lingual cingulum always present on lower premolars [RI = 0.45]; d1 always one-rooted [RI = 0.65]; distal semilunate-facet asymmetric on the pyramidal [RI = 0.50]; Bremer Index = 2). The *Molassitherium* clade (Fig. 6, node D) is supported by three cranial and two dental homoplastic synapomorphies (occipital side inclined backward, [RI = 0.33] short nasal bones [RI = 0.33], and occipital crest forked [RI = 0.22]; crochet always absent on upper molars [RI = 0.69] and mesostyle present on M2 [RI = 0.44]; Bremer Index = 3). *Molassitherium delemontense* differs from *M. albigense* by having nasals with a forked tip in dorsal view, both a labial cingulum usually present and a transverse metaloph on upper premolars, a lingual bridge and a hypocone stronger than the protocone on P2, a lingual wall on P3–4, a labial cingulum usually absent on upper molars, a long metastyle on M1–2, somewhat distinct ectoloph and metaloph on M3; and also by lacking any constricted metaconid and by having a protoconid fold on the lower milk teeth. Node E joins *Mesaceratherium* and remnant Rhinocerotidae with *M. pauliacense* as a sister group to [*M. welcommi*, *M. gaimersheimense*], as in Antoine *et al.* (2010). It is supported by six synapomorphies, among which the crochet always present on the upper molars [RI = 0.69], the posterior groove absent on the ectometaloph of M3 [RI = 0.86], and the lozenge-like dorsal outline of the navicular [RI = 0.44] are the less homoplastic. The *Mesaceratherium* clade (Fig. 6, node F) is not well supported, with only two postcranial synapomorphies (posterior McIII-facet always present on the McII [RI = 0.63] and posterior MtII-facet absent on the MtIII [RI = 0.40]; Bremer Index = 1), while two dental reversals support sister group relationships between *M. welcommi* and *M. gaimersheimense* (presence of a lingual bridge on P4 [RI = 0.33] and labial cingulum always present on upper molars [RI = 0.63]; Bremer Index = 2). The next internal node (Fig. 6, node G), supported by four dental synapomorphies (joined roots on cheek teeth [RI = 0.60]; crochet usually absent on P2–4 [RI = 0.83]; antecrochet usually present on P4 [RI = 0.67]; hypolophid oblique on lower molars [RI = 0.70]; Bremer Index = 4), separates the strongly supported clade *Pleuroceros* (Fig. 6) from more derived Rhinocerotinae, as in Antoine *et al.* (2010). The monophyly of *Pleuroceros* (node H; Bremer Index > 5) is strongly supported by eight unambiguous synapomorphies, the less homoplastic of which are the antecrochet always present on P4 [RI = 0.67], the U-shaped external groove on the lower cheek teeth [RI = 0.57], the presence of a vestigial McV [RI = 0.82] and the salient insertion of the m. extensor carpalis on the metacarpals [RI = 0.70]. Four dental and four postcranial synapomorphies (crochet usually present on P2–4 [RI = 0.83], protoloph interrupted on P2 [RI =

0.54], antecrochet usually present on upper molars [RI = 0.69] and constricted metaconid on lower milk teeth [RI = 0.25]; posteroproximal semilunate-facet absent on the scaphoid [RI = 0.5]; astragalus with trochlea and distal articulation sharing a same axis [RI = 0.73], the expansion of the calcaneus-facet 1 always wide and low [RI = 0.27] and calcaneus-facets 2 and 3 usually independent [RI = 0.52]) support *Protaceratherium minutum* as sister taxon to a clade formed by *Plesiaceratherium mirallesi*, *Aceratheriini* and *Rhinocerotini* (Bremer Index = 4; Fig. 6, node I). *Plesiaceratherium mirallesi* shares 11 synapomorphies with the clade *Aceratheriini* + *Rhinocerotini* (Bremer Index = 4; Fig. 6, node J), such as a low zygomatic arch (RI = 0.70), a triangular M3 in occlusal view (RI = 1), lower cheek teeth with a rounded trigonid (RI = 0.75) and kidney-like condylar facets on the atlas (RI = 1). The clade *Aceratheriini* + *Rhinocerotini* is well supported, with eight unambiguous synapomorphies and a Bremer Index > 5 (Fig. 6, node K). *Aceratheriini* consist of [*Alicornops simorrense* [*Hoploaceratherium tetractylum*, *Aceratherium incisivum*]] (seven to nine synapomorphies; Bremer indices ≥ 4 ; Fig. 6, node L), while *Rhinocerotini* (Fig. 6, node M) include *Teleocerotina* ([*Teleoceras fossiger*, *Prosantorhinus douvillei*]; 23 synapomorphies; Bremer Index > 5; Fig. 6, node N) and *Rhinocerotina* ([*Lartetotherium sansaniense* [[*Dicerorhinus sumatrensis*, *Diceros bicornis*] [*Rhinoceros unicornis*, *R. sondaicus*]]]; node O). All the clades within *Rhinocerotina* are robust and the corresponding branching sequence is consistent with that of Antoine *et al.* (2010), with the one-horned fossil rhino *Lartetotherium sansaniense* being sister group to the *Rhinoceros* and ‘two-horned rhinos’ clades (Fig. 6). Detailing the distribution of synapomorphies within *Aceratheriini* and *Rhinocerotini* is beyond the scope of the present article.

Ghost lineages are inferred within *Rhinocerotinae* (Fig. 7), due to the absence in the present taxonomic sampling of early terminals such as the earliest representative of *Plesiaceratherium* (*P. naricum*, earliest Miocene of Pakistan; Antoine *et al.* 2010), the teleocerotine *Diaceratherium massiliae* (MP26, early Late Oligocene; Ménouret & Guérin 2009) or the late Miocene two-horned rhinocerotines *Stephanorhinus pikermiensis* and *Ceratotherium neumayri* (e.g. Heissig 1999; Antoine & Saraç 2005). Including these taxa has no consequence on the topology of the parsimonious tree but lowers the Consistency Index.

Conclusion

Given the topology of the most parsimonious tree and the strong support of all nodes (24 synapomorphies; $2 \leq$ Bremer Indices ≤ 4), the referral of ‘*Acerotherium albigense* Roman, 1912’ to the genus *Protaceratherium* Abel, 1910, can be discounted. On the other hand, the small hornless rhinocerotid from the ‘middle’ Oligocene

of Europe forms a well-supported clade with the Delémont rhinocerotid, described here, which leads us to propose a new monophyletic genus, *Molassitherium* gen. nov., encompassing the two taxa under the names *M. albigense* (Roman, 1912) comb. nov. and *M. delemontense* sp. nov. *Molassitherium* gen. nov. is clearly distinct from coeval but less derived rhinocerotids such as *Ronzotherium filholi*, *Epiaceratherium bolcense* and *E. magnum*, from the more derived (and younger) representatives of *Mesaceratherium*, *Pleuroceros* and *Plesiaceratherium*, as well as from *Protaceratherium minutum* (the type species of *Protaceratherium*).

Also, this work highlights the mistaken identifications for a decade of ‘*Epiaceratherium magnum* Uhlig, 1999’, because the genus *Epiaceratherium* obviously appears as paraphyletic in the cladogram. Following the principle of priority, this implies that *Epiaceratherium* can be considered as a monospecific genus for the type species *E. bolcense* Abel, 1910, whereas ‘*Epiaceratherium magnum* Uhlig, 1999’ should be assigned to a new genus *incertae sedis*.

Acknowledgements

We thank Maëva J. Orliac for fruitful discussion on morphological character sampling strategy and phylogeny, and Marguerite Huguency for informative discussions about the biochronological context of European Oligocene faunas. We are grateful to Loïc Costeur (Naturhistorisches Museum Basel, Switzerland) and Yves Laurent (Muséum d’Histoire naturelle de Toulouse, France) for access to collections, as well Gaëtan Rauber and the technical crew of the Section d’archéologie et paléontologie (Porrentruy, Switzerland) for field and laboratory work. We are indebted to Jean-Pierre Berger, Loïc Bocat, Jean-Paul Billon-Bruyat, Bastien Mennecart and Laureline Scherler for helpful discussions. The photographs were taken by Bernard Migy (Poillat, Kleinblauen) and Bastien Mennecart (Monclar-de-Quercy). The figures accompanying the photographed specimens were executed by Tayfun Yilmaz. DB’s research is funded by the Swiss National Science Foundation (SNSF, projects 200021-115995 and 200021-126420), the Swiss Federal Roads Authority and the Office de la culture (Canton Jura, Switzerland). OM’s research is supported by the Chinese Natural Science Foundation (No. 41050110135) and a Research Fellowships for International Young Researchers of the Chinese Academy of Sciences (No. 2009Y2BZ3).

Supplementary material

Supplementary material available online DOI: 10.1080/14772019.2012.699007

References

- Abel, O. 1910. Kritische Untersuchungen über die paläogenen Rhinocerotiden Europas. *Abhandlungen der Geologische Reichsanstalt, Wien*, **20**, 1–52.
- Antoine, P.-O. 1997. *Aegyrcitherium beonensis* nov. gen. nov. sp., nouvel élasmothère (Mammalia, Rhinocerotidae) du gisement miocène (MN 4b) de Montréal-du-Gers (Gers, France). Position phylogénétique au sein des Elasmotheriini. *Neues Jahrbuch für Geologie und Paläontologie, Abhandlungen*, **204**, 399–414.
- Antoine, P.-O. 2002. Phylogénie et évolution des Elasmotheriina (Mammalia, Rhinocerotidae). *Mémoires du Muséum National d’Histoire Naturelle*, **188**, 1–359.
- Antoine, P.-O. 2003. Middle Miocene elasmotheriine Rhinocerotidae from China and Mongolia: taxonomic revision and phylogenetic relationships. *Zoologica Scripta*, **32**, 95–118.
- Antoine, P.-O. 2012. Pleistocene and Holocene rhinocerotids (Mammalia, Perissodactyla) from the Indochinese Peninsula. *Comptes Rendus Palevol*, **11**, 159–168. doi:10.1016/j.crpv.2011.03.002
- Antoine, P.-O. & Saraç, G. 2005. The late Miocene mammalian locality of Akkasdagi, Turkey: Rhinocerotidae. *Geodiversitas*, **27**, 601–632.
- Antoine, P.-O. & Welcomme, J.-L. 2000. A new rhinoceros from the Bugti Hills, Baluchistan, Pakistan: the earliest elasmotheriine. *Palaeontology*, **43**, 795–816.
- Antoine, P.-O., Duranthon, F. & Tassy, P. 1997. L’apport des grands mammifères (Rhinocerotidés, Suoidés, Proboscidiens) à la connaissance des gisements du Miocène d’Aquitaine (France). *Mémoires et Travaux de l’Ecole Pratique des Hautes Etudes, Institut de Montpellier*, **21**, 581–590.
- Antoine, P.-O., Bulot, C. & Ginsburg, L. 2000. Une faune rare de rhinocerotidés (Mammalia, Perissodactyla) dans le Miocène inférieur de Pellecatus (Gers, France). *Geobios*, **33**, 249–255.
- Antoine, P.-O., Ducrocq, S., Marivaux, L., Chaimanee, Y., Crochet, J.-Y., Jaeger, J.-J. & Welcomme, J.-L. 2003a. Early rhinocerotids (Mammalia, Perissodactyla) from South Asia and a review of the Holarctic Paleogene rhinocerotid record. *Canadian Journal of Earth Sciences*, **40**, 365–374.
- Antoine, P.-O., Duranthon, F. & Welcomme, J.-L. 2003b. *Alicornops* (Mammalia, Rhinocerotidae) dans le Miocène supérieur des Collines Bugti (Balouchistan, Pakistan): implications phylogénétiques. *Geodiversitas*, **25**, 575–603.
- Antoine, P.-O., Duranthon, F., Hervet, S. & Fleury, G. 2006. Vertébrés de l’Oligocène terminal (MP30) et du Miocène basal (MN1) du méso de Toulouse (SW de la France). *Comptes Rendus Palevol*, **5**, 875–884.
- Antoine, P.-O., Downing, K. F., Crochet, J.-Y., Duranthon, F., Flynn L. J., Marivaux, L., Métais, G., Rajpar A. R. & Roohi, G. 2010. A revision of *Aceratherium blanfordi* Lydekker, 1884 (Mammalia: Rhinocerotidae) from the Early Miocene of Pakistan: postcranials as a key. *Zoological Journal of the Linnean Society*, **160**, 139–194.
- Antoine, P.-O., Métais, G., Orliac, M. J., Peigné, S., Rifaï, S., Solé, F. & Vianey-Liaud, M. 2011. A new late early Oligocene vertebrate fauna from Moissac, SW France. *Comptes Rendus Palevol*, **10**, 239–250.
- Aymard, A. 1854. Des terrains fossilifères du bassin supérieur de la Loire. *Comptes Rendus de l’Académie des Sciences, Paris*, **38**, 673–677.
- Bahlo, E. 1976. Gebissreste von Cricetiden und Theridomyiden (Rodentia) aus dem Mitteloligozaen von Gabsheim bei Alzey

- (Rheinessen). *Mainzer Geowissenschaften Mittheillungen*, **5**, 5–11.
- Barbour, E. H.** 1906. Notice of a new Miocene rhinoceros, *Diceratherium arikareense*. *Science, New Series*, **24**, 780–781.
- Becker, D.** 2009. Earliest record of rhinocerotoids (Mammalia: Perissodactyla) from Switzerland: Systematics and biostratigraphy. *Swiss Journal of Geosciences*, **102**, 375–390.
- Becker, D., Bürgin, T., Oberli, U. & Scherler, L.** 2009. A juvenile skull of *Diaceratherium lemanense* (Rhinocerotidae) from the Aquitanian of Eschenbach (eastern Switzerland). *Neues Jahrbuch für Geologie und Paläontologie, Abhandlungen*, **254**, 5–39.
- Berger, G.** 2008. Die fossilen Schlafmäuse (Gliridae, Rodentia, Mammalia) aus süddeutschen Spaltenfüllungen des Obereozäns und Unteroligozäns. *Münchner Geowissenschaftliche Abhandlungen Reihe A, Geologie und Paläontologie*, **41**, 1–128.
- BiochroM'97.** 1997. Synthèse et tableaux de corrélations. *Mémoires et Travaux de l'École Pratique des Hautes Etudes, Institut de Montpellier*, **21**, 769–805.
- Blainville, H.-M. D. de** 1839–1864. *Ostéographie ou description iconographique comparée du squelette et du système dentaire des mammifères récent et fossiles pour servir de base à la zoologie et à la géologie. Third Volume*. Baillière, Paris.
- Bonis, L. de** 1973. Contribution à l'étude des mammifères de l'Aquitainien de l'Agenais. Rongeurs-Carnivores-Périsodactyles. *Mémoires du Muséum National d'Histoire Naturelle*, **28**, 1–192.
- Bremer, K.** 1994. Branch support and tree stability. *Cladistics*, **10**, 295–304.
- Breuning, S. von** 1924. Beiträge zur Stammesgeschichte der Rhinocerotidae. *Verhandlungen der Zoologisch-Botanischen Gesellschaft in Wien*, **73**, 5–46.
- Brunet, M.** 1979. *Les grands mammifères chefs de file de l'immigration oligocène et le problème de la limite Eocène-Oligocène en Europe*. Fondation Singer-Polignac, Paris, 281 pp.
- Cerdeño, E.** 1995. Cladistic analysis of the Family Rhinocerotidae (Perissodactyla). *American Museum Novitates*, **3143**, 1–25.
- Cerdeño, E. & Sánchez, B.** 2000. Intraspecific variation and evolutionary trends of *Alicornops simorreense* (Rhinocerotidae) in Spain. *Zoologica Scripta*, **29**, 275–305.
- Cope, E. D.** 1878. Descriptions of new extinct Vertebrata from the upper Tertiary and Dakota formations. *Bulletin of the United States Geological and Geographical Survey Territories*, **4**, 379–396.
- Cope, E. D.** 1887. The Perissodactyla. *American Naturalist*, **21**, 985–1007.
- Crusafont, M., Villalta, J. F. & Truyols, J.** 1955. El Burdigaliense continental de la Cuenca del Vallés-Penedés. *Memorias y Comunicaciones del Instituto Geológico de Barcelona, Barcelona*, **12**, 1–272.
- Cuvier, G.** 1822. *Recherches sur les ossements fossiles. 2nd edition. Volume 5*. Edmond d'Ocagne, Paris, 435 pp.
- Dal Piaz, G.** 1930. I Mammiferi dell'Oligocene veneto, *Trigonias ombonii*. *Memorias dell' Instituto Geologico dell' Universita di Padova*, **9**, 2–63.
- Desmarest, A. G.** 1822. *Mammalogie ou description des espèces de mammifères*. Encyclopédie méthodique no. 126, Agasse, Paris, 556 pp.
- Dietrich, W. O.** 1931. Neue Nashornreste aus Schwaben (*Diaceratherium tomerdingensis* n. g. n. sp.). *Zeitschrift für Säugetierkunde*, **6**, 203–220.
- Dollo, L.** 1885. Rhinocéros vivants et fossiles. *Revue des Questions Scientifiques*, **17**, 293–300.
- Duvernoy, G. L.** 1853. Nouvelles études sur les rhinocéros fossiles. *Archives du Muséum d'Histoire Naturelle*, **7**, 1–144.
- Engesser, B. & Mödden, C.** 1997. A new version of the biozonation of the lower freshwater molasse (Oligocene and Agenian) of Switzerland and Savoy on the basis of fossil mammals. *Mémoires et Travaux de l'École Pratique des Hautes Etudes, Institut de Montpellier*, **21**, 475–499.
- Falconer H. & Cautley, P. T.** 1846–1849. *Fauna antiqua sivalensis, being the fossil zoology of the Sewalik Hills, in the north of India*. Smith, Elder & Co., London, 67 pp.
- Farris, J. S.** 1988. Hennig86 reference. Version 1.5. Port Jefferson Station, New York (software).
- Fischer von Waldheim, G. F.** 1814. *Zoögnosia tabulis synopticis illustrate, in usum Paeselectionum Academiae Imperialis Medicochirurgiae*. Nicolai Sergeidis Vsevolozsky, Moscow, 732 pp.
- Forster-Cooper, C.** 1934. XIII. The extinct rhinoceroses of Baluchistan. *Philosophical Transactions of the Royal Society of London, Series B*, **223**, 569–616.
- Göhllich, U.** 1992. *Geologisch-paläontologische Untersuchungen im Nordost-Teil der Murnauer Mulde*. Unpublished Masters thesis, Paläontologie & Geobiologie, Department für Geo- und Umweltwissenschaften, Ludwig-Maximilians-Universität, München.
- Gray, J. E.** 1821. On the natural arrangements of vertebrate animals. *London Medical Repository*, **15**, 296–310.
- Guérin, C.** 1980. Les Rhinocéros (Mammalia, Perissodactyla) du Miocène terminal au Pléistocène supérieur en Europe occidentale. Comparaison avec les espèces actuelles. *Documents du Laboratoire de Géologie de l'Université de Lyon, Sciences de la Terre*, **79**(1–3), 1–1185.
- Hardenbol, J., Thierry, J., Farley, M., Jacquin, T., de Graciansky, P.-C. & Vail, P. R.** 1998. Mesozoic and Cenozoic sequence chronostratigraphic framework of European basins. *Society of Economic Paleontologists and Mineralogists, Special Publication*, **60**, 3–13, 763–78.
- Heissig, K.** 1969. Die Rhinocerotidae (Mammalia) aus der oberoligozänen Spaltenfüllung von Gaimersheim. *Abhandlungen der Bayerischen Akademie der Wissenschaften, Mathematisch-Naturwissenschaftliche Klasse*, **138**, 1–133.
- Heissig, K.** 1973. Die Unterfamilien und Tribus der rezenten und fossilen Rhinocerotidae (Mammalia). *Säugetierkunde Mitteilungen*, **21**, 25–30.
- Heissig, K.** 1989. The Rhinocerotidae. Pp. 399–417 in D. R. Prothero & R. M. Schoch (eds) *The Evolution of Perissodactyla*. Oxford University Press, New York.
- Heissig, K.** 1999. 16. Family Rhinocerotidae. Pp. 175–188 in G. E. Rössner & K. Heissig (eds) *The Miocene Land Mammals of Europe*. Verlag Dr. Friedrich Pfeil, Munich.
- Hugueney, M.** 1984. Theridomys truci de l'Oligocène de Saint-Martin-de-Castillon (Vaucluse, France), nouvelle espèce du genre Theridomys (Rodentia, Mammalia) et sa relation avec la lignée de Theridomys lembronicus. *Scripta Geologica*, **104**, 115–127.
- Hugueney, M. & Guérin, C.** 1981. La faune de mammifères de l'Oligocène moyen de Saint-Menoux (Allier). 2e partie: Marsupiaux, Chiroptères, Carnivores, Périsodactyles, Artiodactyles (Mammalia). *Revue scientifique du Bourbonnais*, **1981**, 52–71.
- Hünemann, K. A.** 1989. Die Nashornskelette (*Aceratherium incisivum* Kaup 1832) aus dem Jungtertiär vom Höwenegg im Hegau (Südwestdeutschland). *Andrias*, **6**, 5–116.
- Hrubesch, K.** 1957. Paracricetodon dehmi, n. sp., ein neuer Nager aus dem Oligocän Mitteleuropas. *Neues Jahrbuch für Geologie und Paläontologie Abhandlungen*, **105**, 250–271.

- Kaup, J. J.** 1832. *Description d'Ossements fossiles de Mammifères inconnus jusqu'à présent, qui se trouvent au Musée grand-ducal de Darmstadt*, pp 49–61. J. G. Heyer, Darmstadt.
- Klaits, B. G.** 1973. Upper Miocene rhinoceroses from Sansan (Gers), France: the manus. *Journal of Paleontology*, **47**, 315–326.
- Lartet, E.** 1837. Note sur les ossements fossiles des terrains tertiaires de Simorre, de Sansan, etc., dans le département du Gers, et sur la découverte récente d'une mâchoire de singe fossile. *Comptes Rendus de l'Académie des Sciences*, **4**, 85–93.
- Lartet, E.** 1851. *Notice sur la colline de Sansan*. Portes, Auch, 47 pp.
- Laudet, F. & Antoine, P.-O.** 2004. Des chambres de population de Dermestidae (Insecta: Coleoptera) sur un os de mammifère tertiaire (phosphorites du Quercy). Implications taphonomiques et paléoenvironnementales. *Geobios*, **37**, 376–381.
- Legendre, S. & Lévêque, F.** 1997. Etalonnage de l'échelle biochronologique mammalienne du Paléogène d'Europe occidentale: vers une intégration à l'échelle globale. *Mémoires et Travaux de l'Ecole Pratique des Hautes Etudes, Institut de Montpellier*, **21**, 461–474.
- Leidy, J.** 1851. Remarks on *Oreodon priscus* and *Rhinoceros occidentalis*. *Proceedings of the Academy of Natural Sciences of Philadelphia*, **5**, 276.
- Leidy, J.** 1871. Report on the vertebrate fossils of the Tertiary formations of the West. *Annals and Reports of the United States Geological and Geographic Survey*, **2**, 340–370.
- Lihoreau, F., Ducrocq, S., Antoine, P.-O., Vianey-Liaud, M., Rifaÿ, S., Garcia, G. & Valentin, X.** 2009. First complete skulls of *Elomeryx crispus* (Gervais, 1849) and of *Protaceratherium albigense* (Roman, 1912) from a new Oligocene locality near Moissac (SW France). *Journal of Vertebrate Paleontology*, **29**, 242–253.
- Lindsay, E. H., Flynn, L. J., Cheema, I. U., Barry, J. C., Downing, K. F., Rajpar, A. R. & Raza, S. M.** 2005. Will Downs and the Zinda Pir Dome. *Palaeontologia Electronica*, **8**, 1–19.
- Linnaeus, C.** 1758. *Systema Naturae per regna tria naturae, secundum classes, ordines, genera, species, cum characteribus, differentiis, synonymis, locis. Regnum animale. 10th edition. Volume 1*. Holmiæ (Salvius), Stockholm, 824 pp.
- Lucas, F. A.** 1900. A new rhinoceros, *Trigonias osborni*, from the Miocene of South Dakota. *United States National Museum Proceedings*, **23**, 221–224.
- Luterbacher, H. P., Ali, J. R., Brinkhuis, H., Gradstein, F. M., Hooker, J. J., Monechi, S., Ogg, J. G., Powell, J., Röhl, U., Sanfilippo, A. & Schmitz, B.** 2004. The Paleogene period. Pp. 384–408 in F. M. Gradstein, J. G. Ogg & A. G. Smith (eds) *A geologic time scale*. Cambridge University Press, Cambridge.
- Lydekker, R.** 1884. Additional Siwalik Perissodactyla and Proboscidea. *Memoirs of the Geological Survey of India - Palaeontologia Indica*, **3**, 1–34.
- Marsh, O. C.** 1875. Notice of new Tertiary mammals. IV. *American Journal of Sciences and Arts*, **109**, 239–250.
- Ménouret, B. & Guérin, C.** 2009. *Diaceratherium massiliae* nov. sp. des argiles oligocènes de Saint-André et Saint-Henri à Marseille et de Les Milles près d'Aix-en-Provence (SE de la France), premier grand Rhinocerotidae brachypode européen. *Geobios*, **42**, 293–327.
- Muratet, B., Duranthon, F., Lange-Badré, B. & Riveline, J.** 1992. Discontinuité d'origine eustatique dans les molasses oligocènes du Bassin aquitain (SW France). Apport de la biochronologie. *Comptes Rendus de l'Académie des Sciences, Paris*, **315**, 1113–1118.
- Orliac, M. J., Antoine P.-O. & Ducrocq, S.** 2010. Phylogenetic relationships of the Suidae (Mammalia, Cetartiodactyla): new insights on the relations within Suoidea. *Zoologica Scripta*, **39**, 315–330.
- Osborn, H. F.** 1900. Phylogeny of rhinoceroses of Europe. *Memoirs of the American Museum of Natural History*, **13**, 229–267.
- Owen, R.** 1848. *On the archetype and homologies of the vertebrate skeleton*. J. Van Voorst, London, 203 pp.
- Picot, L., Becker, D., Cavin, L., Pirkenseer, C., Lapaire, F., Rauber, G., Hochuli, P. A., Spezzaferrri, S. & Berger, J.-P.** 2008. Sédimentologie et paléontologie des paléoenvironnements côtiers rupéliens de la Molasse marine rhénane dans le Jura suisse. *Swiss Journal of Geosciences*, **101**, 483–513.
- Pilgrim, G. E.** 1912. The vertebrate fauna of the Gaj Series in the Bugti Hills and the Punjab. *Paleontologia Indica*, **4**, 1–83.
- Prothero, D. R.** 1998. 42. Rhinocerotidae. Pp. 595–605 in C. M. Janis, K. M. Scott & L. L. Jacobs (eds) *Evolution of Tertiary mammals of North America. Volume 1, Terrestrial carnivores, ungulates and ungulate-like mammals*. Cambridge University Press, New York.
- Prothero, D. R.** 2005. *The Evolution of North American Rhinoceroses*. Cambridge University Press, Cambridge, 218 pp.
- Prothero, D. R., Manning, E. & Hanson, C. B.** 1986. The phylogeny of the Rhinocerotidae (Mammalia, Perissodactyla). *Zoological Journal of the Linnean Society*, **87**, 341–366.
- Richard, M.** 1937. Une nouvelle espèce de Rhinocerotidés aquitain: *Diaceratherium pauliacensis*. *Bulletin de la Société d'Histoire Naturelle de Toulouse*, **71**, 165–170.
- Roger, O.** 1898. Wirbeltierreste aus dem Dinotheriensande der bayerisch-schwäbischen Hochebene. *Bericht des Naturwissenschaftlichen Vereins für Schwaben*, **33**, 1–46, 383–396.
- Roman, F.** 1912. Les rhinocerotidés de l'Oligocène d'Europe. *Archives du Musée des Sciences Naturelles de Lyon*, **11**, 1–92.
- Roman, F.** 1924. Contribution à l'étude de la faune de mammifères des Littorinenkalk (Oligocène supérieur) du Bassin de Mayence. *Travaux du Laboratoire de Géologie de la Faculté des Sciences de Lyon*, **7**, 1–55.
- Saraç, G.** 2003. Discovery of *Protaceratherium albigense* (Rhinocerotidae, Mammalia) in Oligocene coastal deposits of Turkish Thrace. *Deinsea*, **10**, 509–517.
- Schaub, S.** 1925. Die hamsterartigen Nagetiere des Tertiärs und ihre lebenden Verwandten. Eine systematisch-odontologische Studie. *Abhandlungen der schweizerischen paläontologischen Gesellschaft*, **45**, 1–114.
- Schmidt-Kittler, N., Brunet, M., Godinot, M., Franzen, J. L., Hooker, J. J., Legendre, S. & Vianey-Liaud, M.** 1987. European reference levels and correlation tables. *Münchner Geowissenschaftliche Abhandlungen Reihe A, Geologie und Paläontologie*, **10**, 13–31.
- Scott, W. B.** 1941. Perissodactyla. The mammalian fauna of the White River Oligocene. *Transactions of the American Philosophical Society*, **28**, 747–980.
- Simpson, G. G.** 1945. The principles of classification and a classification of mammals. *Bulletin of the American Museum of Natural History*, **85**, 1–350.
- Spillmann** 1969. Neue Rhinocerotiden aus den oligozänen Sanden des Linzer Beckens. *Jahrbuch des Oberösterreichischen Musealvereines*, **114**, 201–254.

- Swofford, D. L.** 2002. *PAUP*. Phylogenetic Analysis Using Parsimony (*and Other Methods). Version 4*. Sinauer Associates, Sunderland, Massachusetts. [software]
- Tanner, L. G.** 1969. A new rhinoceros from the Nebraska Miocene. *Bulletin of the University of Nebraska State Museum*, **8**, 395–412.
- Thaler, L.** 1969. Rongeurs nouveaux de l'Oligocène moyen d'Espagne. *Palaeovertebrata*, **2**, 191–207.
- Uhlig, U.** 1999. Die Rhinocerotidae (Mammalia) aus der unteroligozänen Spaltenfüllung Möhren 13 bei Treuchtlingen in Bayern. *Abhandlungen der Bayerischen Akademie der Wissenschaften, Mathematisch-Naturwissenschaftliche Klasse, Neue Folge*, **170**, 1–254.
- Uhlig, U.** 2001. The Gliridae (Mammalia) from the Oligocene (MP24) of Gröben 3 in the folded molasse of southern Germany. *Palaeovertebrata*, **30**, 151–187.
- Vianey-Liaud, M.** 1972. L'évolution du genre *Theridomys* à l'Oligocène moyen. Intérêt biostratigraphique. *Bulletin du Muséum national d'Histoire naturelle*, **98**, 295–372.
- Vianey-Liaud, M.** 1998. La radiation des Theridomyidae (Rodentia) à l'Oligocène inférieur : modalités et implications biochronologiques. *Geologica et Palaeontologica*, **32**, 253–285.
- Vianey-Liaud, M. & Michaux, J.** 2003. Évolution « graduelle » à l'échelle géologique chez les rongeurs fossiles du Cénozoïque européen. *Comptes Rendus Palevol*, **2**, 455–472.
- Vianey-Liaud, M. & Schmid, B.** 2009. Diversité, datation et paléoenvironnement de la faune de mammifères oligocène de Cavalé (Quercy, SO France): contribution de l'analyse morphométrique des Theridomyinae (Mammalia, Rodentia). *Geodiversitas*, **31**, 909–941.
- Wermelinger, M.** 1998. *Prosantorhinus cf. douvillei* (Mammalia, Rhinocerotidae), petit rhinocéros du gisement miocène (MN 4b) de Montréal-du-Gers (Gers, France). *Etude ostéologique du membre thoracique*. Unpublished PhD, University Toulouse III.
- Wood, H. E.** 1927. Some early Tertiary rhinoceroses and hyracodonts. *Bulletin of the American Paleontologists*, **13**, 165–249.
- Wood, H. E.** 1932. Status of *Epiaceratherium* (Rhinocerotidae). *Journal of Mammalogy*, **13**, 169–170.
- Yan, D. & Heissig, K.** 1986. Revision and autopodial morphology of the Chinese-European Rhinocerotid genus *Plesiaceratherium* Young 1937. *Zitteliana Abhandlungen der Bayerische Staatssammlung für Paläontologie und historisches Geologie*, **14**, 81–110.
- Young, C.-C.** 1937. On a Miocene mammalian fauna from Shantung. *Bulletin of the Geological Society of China*, **17**, 209–245.
3. *Nasal/lacrymal: contact*: (0) long; (1) punctual or absent.
 4. *Zygomatic arch*: (0) low; (1) high; (2) very high.
 5. *Zygomatic arch: processus postorbitalis*: (0) present; (1) absent.
 6. *Zygomatic arch: processus postorbitalis*: (0) on jugal; (1) on squamosal.
 7. *Jugal/squamosal: suture*: (0) smooth; (1) rugose.
 8. *Skull: dorsal profile*: (0) flat; (1) concave; (2) very concave.
 9. *Sphenoid: foramina sphenorbitale & rotundum*: (0) distinct; (1) fused (foramen ovale).
 10. *Squamosal: area between temporal and nuchal crests*: (0) flat; (1) depression.
 11. *External auditory pseudo-meatus*: (0) open; (1) partly closed; (2) totally closed (circular).
 12. *Occipital side*: (0) inclined forward; (1) vertical; (2) inclined backward.
 13. *Occipital: nuchal tubercle*: (0) small; (1) developed; (2) much developed.
 14. *Pterygoid: posterior margin*: (0) nearly horizontal; (1) nearly vertical.
 15. *Skull*: (0) dolichocephalic; (1) brachycephalic.
 16. *Nasal bones: rostral end*: (0) narrow; (1) broad; (2) very broad.
 17. *Nasal bones*: (0) totally separated; (1) anteriorly separated; (2) fused.
 18. *Nasal bones*: (0) long; (1) short; (2) very long.
 19. *Median nasal horn*: (0) absent; (1) present.
 20. *Median nasal horn*: (0) small; (1) large.
 21. *Paired nasal horns*: (0) terminal bumps; (1) lateral crests.
 22. *Frontal horn*: (0) absent; (1) present.
 23. *Frontal-parietal*: (0) sagittal crest; (1) close fronto-parietal crests; (2) distant crest.
 24. *Occipital crest*: (0) concave; (1) straight; (2) forked.
 25. *Maxilla: processus zygomaticus maxillari*: (0) progressive; (1) brutal.
 26. *Vomer*: (0) sharp; (1) rounded.
 27. *Squamosal: articular tubercle*: (0) smooth; (1) sharp, carinated.
 28. *Squamosal: transversal profile of the articular tubercle*: (0) straight; (1) concave.
 29. *Squamosal: processus postglenoidalis (articulation, in cross section)*: (0) flat; (1) convex; (2) right dihedron.
 30. *Basioccipital: sagittal crest on the basilar process*: (0) absent; (1) present.
 31. *Squamosal: posterior groove on the processus zygomaticus*: (0) absent; (1) present.
 32. *Squamosal-occipital: processus posttympanicus and processus paraoccipitalis*: (0) fused; (1) distant.
 33. *Squamosal: processus posttympanicus*: (0) well-developed; (1) little-developed; (2) huge.

Appendix 1. Morphological characters used in the phylogenetic analysis. The list corresponds to the 214 characters included in the list proposed by Antoine (2003) and Antoine *et al.* (2003b).

Cranial characters

1. *Maxilla: foramen infraorbitalis*: (0) above pre-molars; (1) above molars.
2. *Nasal septum*: (0) never ossified; (1) ossified (sometimes->always).

34. *Occipital: foramen magnum*: (0) circular; (1) subtriangular.
35. *Basioccipital: median ridge on the condyle*: (0) absent; (1) present.
36. *Basioccipital: median truncation on the condyle*: (0) absent; (1) present.

Mandibular characters

37. *Symphysis (orientation)*: (0) very upraised; (1) upraised; (2) nearly horizontal; (3) sloping down.
38. *Symphysis*: (0) spindly; (1) massive; (2) very massive.
39. *Corpus mandibulae: lingual groove*: (0) present; (1) absent.
40. *Corpus mandibulae: lingual groove*: (0) still present at adult stage; (1) present at juvenile stage only.
41. *Corpus mandibulae: base*: (0) straight; (1) convex; (2) very convex.
42. *Ramus*: (0) vertical; (1) inclined forward; (2) inclined backward.
43. *Ramus: processus coronoideus*: (0) well-developed; (1) little-developed.
44. *Foramen mandibulare*: (0) below teeth-neck line; (1) above teeth-neck level.

Dental characters

45. *Compared length of P-p/M-m*: (0) $(100 * LP3-4/LM1-3) > 50$; (1) $42 < (100 * LP3-4/LM1-3) < 50$; (2) $(100 * LP3-4/LM1-3) < 42$.
46. *Cheek teeth: cement*: (0) absent; (1) present.
47. *Cheek teeth: aspect of the enamel*: (0) wrinkled; (1) wrinkled and corrugated; (2) corrugated and arborescent.
48. *Cheek teeth: crown*: (0) low; (1) high.
49. *Cheek teeth: roots*: (0) distinct; (1) joined; (2) fused.
50. *I1*: (0) present; (1) absent.
51. *I1: shape of the crown (cross section)*: (0) almond; (1) oval; (2) halfmoon.
52. *I2*: (0) present; (1) absent.
53. *I3*: (0) present; (1) absent.
54. *C*: (0) present; (1) absent.
55. *i1*: (0) present; (1) absent.
56. *i1: crown*: (0) developed, with a pronounced neck; (1) reduced and/or vestigial.
57. *i2: shape*: (0) incisor-like; (1) tusk-like.
58. *i2: orientation*: (0) parallel; (1) diverging rostrally.
59. *i3*: (0) present; (1) absent.
60. *c*: (0) present; (1) absent.
61. *Upper premolars: labial cingulum*: (0) always present; (1) usually present; (2) usually absent; (3) always absent.
62. *P2-4: crochet*: (0) always absent; (1) usually absent; (2) usually present; (3) always present.

63. *P2-4: crochet*: (0) always simple; (1) usually simple; (2) usually multiple.
64. *P2-4: metaloph constriction*: (0) absent; (1) present.
65. *P2-4: lingual cingulum*: (0) always present; (1) usually present; (2) usually absent; (3) always absent.
66. *P2-4: lingual cingulum*: (0) continuous; (1) reduced.
67. *P2-4: postfossette*: (0) narrow; (1) wide; (2) posterior wall.
68. *P2-3: antecrochet*: (0) always absent; (1) usually absent; (2) usually present; (3) always present.
69. *P1 (in adults)*: (0) always present; (1) usually present; (2) usually absent.
70. *P2: protocone and hypocone*: (0) fused; (1) lingual bridge; (2) separated; (3) lingual wall.
71. *P2: metaloph*: (0) hypocone posterior to metacone; (1) transverse; (2) hypocone anterior to metacone.
72. *P2: protocone/hypocone*: (0) equal or stronger; (1) less strong.
73. *P2: protoloph*: (0) present; (1) absent.
74. *P2: protoloph*: (0) joined to the ectoloph; (1) interrupted.
75. *P3-4: constriction of the protocone*: (0) always absent; (1) usually absent; (2) usually present; (3) always present.
76. *P3-4: protocone and hypocone*: (0) fused; (1) lingual bridge; (2) separated; (3) lingual wall.
77. *P3-4: metaloph*: (0) transverse; (1) hypocone posterior to metacone; (2) hypocone anterior to metacone.
78. *P3: protoloph*: (0) joined to the ectoloph; (1) interrupted.
79. *P4: antecrochet*: (0) always absent; (1) usually absent; (2) usually present; (3) always present.
80. *P4: metacone and hypocone*: (0) joined; (1) separated.
81. *Upper molars: labial cingulum*: (0) always present; (1) usually present; (2) usually absent; (3) always absent.
82. *Upper molars: antecrochet*: (0) always absent; (1) usually absent; (2) usually present; (3) always present.
83. *Upper molars: crochet*: (0) always absent; (1) usually absent; (2) usually present; (3) always present.
84. *Upper molars: crista*: (0) always absent; (1) usually absent; (2) usually present; (3) always present.
85. *Upper molars: medifossette*: (0) always absent; (1) usually absent; (2) usually present.
86. *Upper molars: lingual cingulum*: (0) always present; (1) usually present; (2) usually absent; (3) always absent.

87. *M1-2: constriction of the protocone*: (0) always absent; (1) usually absent; (2) usually present; (3) always present.
88. *M1-2: constriction of the protocone*: (0) weak; (1) strong.
89. *M1-2: metacone fold*: (0) present; (1) absent.
90. *M1-2: metastyle*: (0) short; (1) long.
91. *M1-2: metaloph*: (0) long; (1) short.
92. *M1-2: posterior part of the ectoloph*: (0) straight; (1) concave.
93. *M1-2: posterior cingulum*: (0) continuous; (1) low and interrupted.
94. *M1: metaloph*: (0) continuous; (1) hypocone isolated.
95. *M2: protocone, lingual groove*: (0) always absent; (1) usually absent; (2) always present.
96. *M2: metaloph*: (0) continuous; (1) hypocone isolated.
97. *M2: mesostyle*: (0) absent; (1) present.
98. *M3: ectoloph and metaloph*: (0) distinct; (1) fused (ectometaloph).
99. *M3: shape*: (0) quadrangular; (1) triangular.
100. *M3: constriction of the protocone*: (0) always absent; (1) usually absent; (2) always present.
101. *M3: posterior groove on the ectometaloph*: (0) present; (1) absent.
102. *p2-3: vertical external rugosities*: (0) absent; (1) present.
103. *Lower cheek teeth: external groove*: (0) developed; (1) smooth (U-shaped); (2) acute (V-shaped).
104. *Lower cheek teeth: trigonid*: (0) angular; (1) rounded.
105. *Lower cheek teeth: trigonid*: (0) obtuse or right dihedral; (1) acute dihedral.
106. *Lower cheek teeth: metaconid*: (0) joined to the metalophid; (1) constricted.
107. *Lower premolars: lingual opening of the posterior valley (lingual view)*: (0) U-shaped; (1) V-shaped.
108. *Lower premolars: lingual cingulum*: (0) always present; (1) usually present; (2) usually present; (3) always present.
109. *Lower premolars: lingual cingulum*: (0) reduced; (1) continuous.
110. *Lower premolars: labial cingulum*: (0) present; (1) absent.
111. *Lower premolars: labial cingulum*: (0) continuous; (1) reduced.
112. *d1/p1 (in adults)*: (0) always present; (1) usually present; (2) usually absent; (3) always absent.
113. *d1*: (0) always biradicate; (1) usually biradicate; (2) always one-rooted.
114. *p2: paralophid*: (0) isolated, spur-like; (1) curved, without constriction.
115. *p2: posterior valley*: (0) lingually open; (1) usually closed; (2) always closed.
116. *Lower molars: lingual cingulum*: (0) reduced; (1) continuous.
117. *Lower molars: hypolophid*: (0) transverse; (1) oblique; (2) almost mesiodistally oriented.
118. *m2-3: lingual groove of the entoconid*: (0) absent; (1) present.
119. *D2: mesostyle*: (0) present; (1) absent.
120. *D3-4: mesostyle*: (0) absent; (1) present.
121. *D2: secondary folds*: (0) absent; (1) present.
122. *Lower milk teeth: constriction of the metaconid*: (0) present; (1) absent.
123. *Lower milk teeth: protoconid fold*: (0) present; (1) absent.
124. *d2-3: vertical external rugosities*: (0) absent; (1) present.
125. *d2-3: ectolophid fold*: (0) present; (1) absent.
126. *d2: anterior groove on the ectolophid*: (0) absent; (1) present.
127. *d2: paralophid*: (0) simple; (1) double.
128. *d2: posterior valley*: (0) always open; (1) usually open; (2) usually closed; (3) always closed.
129. *d3: lingual groove on the entoconid*: (0) always absent; (1) usually absent; (2) always present.

Postcranial characters

130. *Atlas: outline of the rachidian canal*: (0) bulb; (1) mushroom.
131. *Atlas: alar notch*: (0) absent; (1) present.
132. *Atlas: foramen vertebrae lateralis*: (0) absent; (1) present.
133. *Atlas: condylar facets*: (0) comma-like; (1) kidney-like.
134. *Atlas: axis-facets*: (0) straight; (1) sigmoid; (2) transversally concave.
135. *Atlas: foramen transversarium*: (0) present; (1) absent.
136. *Scapula*: (0) elongated ($1.5 < H/APD < 2$); (1) very elongated ($2 < H/APD$); (2) spatulated ($H/APD < 1.5$).
137. *Scapula: glenoid fossa*: (0) oval; (1) medial border straight.
138. *Humerus: fossa olecrani*: (0) high; (1) low.
139. *Humerus: distal articulation*: (0) egg cup-shaped (shallow median constriction); (1) diabolo-shaped (strong median constriction).
140. *Humerus: scar on the trochlea*: (0) absent; (1) present.
141. *Humerus: distal gutter on the epicondyle*: (0) absent; (1) present.
142. *Radius: anterior border of the proximal articulation*: (0) straight; (1) M-shaped.
143. *Radius: medial border of the diaphysis*: (0) straight; (1) concave.

144. *Radius: proximal ulna-facets*: (0) always separate; (1) usually separate; (2) usually fused; (3) always fused.
145. *Radius: insertion of the m. biceps brachii*: (0) shallow; (1) deep.
146. *Radius/ulna*: (0) independent; (1) in contact or fused.
147. *Radius: gutter for the m. extensor carpi*: (0) deep and wide; (1) weakly developed.
148. *Radius: posterior expansion of the scaphoid-facet*: (0) low; (1) high.
149. *Ulna: angle between diaphysis and olecranon*: (0) open; (1) closed.
150. *Ulna: anterior tubercle on the distal end*: (0) absent; (1) present.
151. *Scaphoid: postero-proximal facet with semilunate*: (0) present; (1) absent or contact.
152. *Scaphoid: trapezium-facet*: (0) large; (1) small.
153. *Scaphoid: magnum-facet in lateral view*: (0) concave; (1) straight.
154. *Scaphoid: comparison between anterior and posterior heights*: (0) equal; (1) antH < postH.
155. *Semilunate: ulna-facet*: (0) absent; (1) present.
156. *Semilunate: anterior side*: (0) keeled; (1) smooth.
157. *Pyramidal: distal facet for semilunate*: (0) symmetric; (1) asymmetric; (2) L-shaped.
158. *Trapezoid: proximal border in anterior view*: (0) symmetric; (1) asymmetric.
159. *Magnum: indentation on the medial side*: (0) absent; (1) present.
160. *Magnum: indentation on the medial side*: (0) always shallow; (1) usually shallow; (2) always deep.
161. *Magnum: posterior tuberosity*: (0) short; (1) long.
162. *Magnum: posterior tuberosity*: (0) curved; (1) straight.
163. *Unciform: pyramidal- and McV-facets*: (0) always separate; (1) usually separate; (2) always in contact.
164. *McII: magnum-facet*: (0) curved; (1) straight.
165. *McII: posterior McIII-facet*: (0) always absent; (1) usually absent; (2) always present.
166. *McII: anterior and posterior McIII-facets*: (0) separated; (1) fused.
167. *McII: trapezium-facet*: (0) always present; (1) usually present; (2) always absent.
168. *McIII: magnum-facet in anterior view*: (0) visible; (1) invisible.
169. *McIV: proximal facet, outline*: (0) trapezoid; (1) pentagonal; (2) triangular.
170. *McV*: (0) functional; (1) vestigial.
171. *Metacarpals: insertion of the m. extensor carpalis*: (0) flat; (1) salient.
172. *Coxal: acetabulum*: (0) oval or subcircular; (1) subtriangular.
173. *Femur: trochanter major*: (0) high; (1) low.
174. *Femur: head*: (0) hemispheric; (1) medially acuminate.
175. *Femur: fovea capitis*: (0) high and narrow; (1) low and wide.
176. *Femur: third trochanter*: (0) developed; (1) very developed.
177. *Femur: angle between the medial lip of the trochlea and the diaphysis*: (0) broken angle; (1) ramp.
178. *Femur: proximal border of the patellar trochlea*: (0) curved; (1) straight.
179. *Tibia: antero-distal groove*: (0) present; (1) absent.
180. *Tibia: medio-distal gutter*: (0) shallow; (1) deep.
181. *Tibia-fibula*: (0) independent; (1) in contact or fused.
182. *Tibia: posterior apophysis*: (0) high; (1) low.
183. *Tibia: posterior apophysis*: (0) acute/sharp; (1) rounded.
184. *Fibula: proximal articulation*: (0) low; (1) high.
185. *Fibula: distal end*: (0) slender; (1) robust.
186. *Fibula: latero-distal gutter (tendon m. peroneus)*: (0) shallow; (1) deep.
187. *Fibula: position of the latero-distal gutter*: (0) posterior; (1) median.
188. *Astragalus: TD/H*: (0) TD/H < 1; (1) 1 < TD/H < 1.2; (2) 1.2 < TD/H.
189. *Astragalus: APD/H*: (0) APD/H < 0.65; (1) 0.65 < APD/H.
190. *Astragalus: orientation of the fibula-facet*: (0) subvertical; (1) oblique.
191. *Astragalus: fibula-facet*: (0) flat; (1) concave.
192. *Astragalus: collum tali*: (0) high; (1) low.
193. *Astragalus: posterior stop on the cuboid-facet*: (0) present; (1) absent.
194. *Astragalus: caudal border of the trochlea, in proximal view*: (0) sinuous; (1) nearly straight.
195. *Astragalus: orientation trochlea/distal articulation*: (0) very oblique; (1) same axis.
196. *Astragalus: expansion of the calcaneus-facet 1*: (0) always present; (1) sometimes absent; (2) always absent.
197. *Astragalus: expansion of the calcaneus-facet 1*: (0) always wide and low; (1) usually wide and low; (2) always high and narrow.
198. *Astragalus: calcaneus-facet 1*: (0) very concave; (1) nearly flat.
199. *Astragalus: calcaneus-facets 2 and 3*: (0) always independent; (1) usually independent; (2) usually fused; (3) always fused.
200. *Calcaneus: fibula-facet*: (0) always absent; (1) usually absent; (2) usually present; (3) always present.
201. *Calcaneus: tibia-facet*: (0) always absent; (1) usually absent; (2) always present.
202. *Calcaneus: tuber calcanei*: (0) massive; (1) slender.

203. *Calcaneus*: insertion of the *m. fibularis longus*: **(0)** salient; **(1)** invisible.
204. *Navicular*: cross section in proximal view: **(0)** lozenge; **(1)** rectangle.
205. *Cuboid*: proximal side: **(0)** oval; **(1)** triangular.
206. *MtIII*: proximal border of the anterior side, anterior view: **(0)** straight; **(1)** concave; **(2)** sigmoid.
207. *MtIII*: posterior *MtII*-facet: **(0)** present; **(1)** absent.
208. *MtIII*: distal widening of the diaphysis (in adults): **(0)** absent; **(1)** present.
209. *MtIII*: cuboid-facet: **(0)** absent; **(1)** present.
210. *MtIV*: postero-proximal tuberosity: **(0)** isolated; **(1)** pad-shaped and continuous.
211. *Phalanx I* for *MtIII*: symmetrical insertions: **(0)** lateral; **(1)** nearly anterior.
212. *Limbs*: **(0)** slender; **(1)** robust (brachypod).
213. *Metapodials*: intermediate reliefs: **(0)** high and acute; **(1)** low and smooth.
214. *Lateral metapodials*: insertion of the *m. interossei*: **(0)** long; **(1)** short.

